

5

Atmospheric aerosols

Rudolf F. Pueschel

- 5.1. INTRODUCTION AND OVERVIEW
 - 5.1.1. Definition
 - 5.1.2. Climate Forcing
 - 5.1.3. Effects on Clouds
 - 5.1.4. Air Pollution
 - 5.1.5. Relevant Aerosol Characteristics
- 5.2. FORMATION, TRANSFORMATION, REMOVAL
 - 5.2.1. Primary and Secondary Aerosols
 - 5.2.2. Meteorological Effects
 - 5.2.3. Emission Rates
 - 5.2.3.1. Man-Made Aerosols
 - 5.2.3.2. Natural Aerosols
 - 5.2.3.3. A Comparison
 - 5.2.4. Transformation
 - 5.2.4.1. Condensation
 - 5.2.4.2. Oxidation and Neutralization
 - 5.2.4.3. Coagulation
 - 5.2.5. Removal
 - 5.2.5.1. Dry Deposition
 - 5.2.5.2. Wet Removal
 - 5.2.6. Residence Times
 - 5.2.7. Size Distributions
 - 5.2.8. Composition
 - 5.2.9. Spatial Distributions
- 5.3. STRATOSPHERIC AEROSOLS
- 5.4. EFFECTS
 - 5.4.1. Climatic Changes
 - 5.4.1.1. Direct Radiative Forcing
 - 5.4.1.2. Indirect Radiative Forcing
 - 5.4.1.3. Stratospheric Aerosol Radiative Forcing

5.4.2. Heterogeneous Chemistry

5.4.2.1. Stratospheric Ozone Depletion

5.4.2.2. Tropospheric Heterogeneous Chemistry

5.5. SUMMARY AND FUTURE NEEDS

Acknowledgments

References

5.1. INTRODUCTION AND OVERVIEW

5.1.1. Definition

Aerosols are defined as particles and/or droplets suspended in air. Some have anthropogenic origin and some are naturally produced. They are generated by the mechanical disintegration of soil and sea-spray yielding primary particles of sizes generally larger than $1\ \mu\text{m}$, and by gas-to-particle conversions that result in submicron secondary aerosols. Although highly variable in space and time, they are always present in the atmosphere.

5.1.2. Climate Forcing

Aerosol and cloud particles exert a variety of important influences on the Earth's climate. Aerosols are part of the Earth-atmosphere climate system because they interact with both incoming solar and outgoing terrestrial radiation. They do this directly through scattering and absorption and indirectly through effects on clouds. The effect of aerosols on long-wave terrestrial (infrared) radiation is much smaller than their interaction with solar energy, because the transparency of aerosols increases at longer wavelengths and because they are most concentrated in the lower troposphere where the air temperature, which governs emissions, is similar to the surface temperature.

Submicrometer aerosols usually predominate in terms of number of particles per unit volume of air. Particles of such a size scatter radiation from the Sun very effectively because they have dimensions close to the wavelengths of visible light. Light absorption is dominated by particles containing elemental carbon (soot) produced by incomplete combustion of fossil fuels and by biomass burning. Light scattering dominates globally, although absorption can be significant at high latitudes. Light absorption lowers the aerosol single-scatter albedo ω_0 , a measure of the fraction of light attenuation (absorption plus scattering) that is due to scattering alone. Whether the aerosol warms or cools the Earth-atmosphere system depends on the magnitude of its single scatter albedo in relation to the surface albedo.

Major volcanic eruptions produce stratospheric aerosols that heat the stratosphere by several degrees Kelvin and are thought to significantly cool the

troposphere (e.g., Laciš et al., 1992). The 1815 eruption of Indonesia's Tambora, the largest on record, is widely believed to have caused June snowstorms and severe crop failures at mid-latitudes during the following "year without summer". The substantially larger eruptions of prehistory call attention to volcanism as an important natural agent of climate change (Sigurdsson and Laj, 1992).

Stratospheric heating and increased aerosol surface area can lead to important dynamical and chemical effects, such as lifting the stratospheric ozone layer via convective motions (Kinne et al., 1992) and causing important changes in ozone destruction rates (Prather, 1992). In the Arctic and Antarctic stratospheres the coldest wintertime temperatures cause nitric acid and water vapor to condense (Toon et al., 1986), forming polar stratospheric clouds (PSCs) that facilitate ozone depletion both by removing nitrogen from the stratosphere (hence curtailing the reaction path that protects ozone from chlorine-catalyzed destruction) and by providing reaction surfaces (which convert chlorine from benign to reactive forms).

In the troposphere, man-made sulfate particles, once thought to have significance only near their urban sources, are now recognized to have global radiative effects (Charlson et al., 1992) that may have significantly offset the warming induced by the greenhouse gases released in industrial times (IPCC, 1990). Most sulfate particles originate from sulfur dioxide (SO_2). The emission of man-made SO_2 had increased to about 150 Tg year^{-1} in 1980 from about 10 Tg year^{-1} in pre-industrial times (World Resources, 1989). Smoke particles from biomass burning have been postulated to produce a similar cooling (Penner et al., 1992), while sulfate particles produced from biogenic dimethylsulfide have been hypothesized to influence albedo, with possible feedback effects on their production (Charlson et al., 1987).

5.1.3. Effects on Clouds

The effects of aerosols on clouds are caused by a small but important subset of aerosol particles called cloud condensation nuclei (CCNs). These are particles with an affinity to water vapor, which condenses upon them preferably, causing clouds to form at supersaturations of a fraction of 1% (Köhler, 1926). Without CCNs, supersaturation of several hundred per cent would occur in the atmosphere before clouds could form. Both the radiative fluxes and the global water cycle under such conditions would be critically different from what they actually are.

The concentration, size, and water solubility of CCNs have an immediate influence on the concentration and size of cloud droplets, which in turn determine the radiative properties of clouds (Twomey, 1977). Physical (coagulation) and chemical (surface adsorption of gases) interactions between natural and

man-made substances can influence the cloud-forming ability of aerosols, thereby affecting the frequency of formation, lifetime, and radiative properties of clouds. At constant water vapor mixing ratios and temperature, increased concentrations of CCNs result in an increased number of cloud droplets of smaller size, thereby enhancing the short-wave albedo of clouds. Anthropogenic sulfate aerosols and smokes from biomass burning dominate man-made albedo increases of clouds. However, soot particles incorporated in sufficient amounts into cloud droplets can reduce cloud albedo (Twohy et al., 1989). In contrast, the perturbation in long-wave absorption by cloud modification is negligible, because tropospheric clouds are already optically thick at infrared wavelengths (Paltridge and Platt, 1976).

An increase in cloud droplet concentration due to a decrease in mean droplet size can inhibit growth to precipitation particle sizes and thus extend cloud lifetimes (e.g., Twomey, 1991). The resultant increase in fractional cloud cover would affect radiation transfer through the atmosphere. Inhibited precipitation development could further alter the amount and distribution of water vapor and heat in the atmosphere and thereby modify the Earth's hydrological cycle. Changes in global weather patterns as well as in the concentration of water vapor, the dominant greenhouse gas, could be the consequence.

5.1.4. Air Pollution

Aerosols play a role in air pollution, defined as the presence in the atmosphere of a substance in such amounts as to adversely affect humans, animals, vegetation, or materials (Williamson, 1973). Chronic exposure to high concentrations of particulate pollutants may be injurious to the lung. In addition, aerosols can play a synergistic role in intensifying the toxic effects of gases such as SO_2 and NO_x , in catalyzing the oxidation of SO_2 to H_2SO_4 , and in increasing atmospheric turbidity and reducing visibility. There are instances of increases in both mortality and morbidity due to particulate air pollutants. Examples include an episode in Belgium's Meuse Valley in 1930 when stagnation of the overlying air caused a build-up of pollutant concentrations during a week-long period. Many people became ill and 60 died. Other episodes are an incident in Donora, Pennsylvania in 1948 when half the population of 14,000 became ill and 20 died, and a "killer fog" in London in 1952 that resulted in 4000 deaths.

The adverse effects of air pollutants are often so insidious that their exact toll is difficult to assess. It has been estimated, however, that the annual loss from damage to crops, plants, trees, and materials in the United States alone may amount to as much as \$5 billion, and that health expenses and lost income due to disease range between \$2 billion and \$6 billion (see Chapter 1).

5.1.5. Relevant Aerosol Characteristics

Aerosol characteristics that determine environmental effects are physical (size, shape, number), chemical (composition), and optical (refractive index) properties. These properties are difficult to assess for a variety of reasons. One of these is the strong variability of aerosol concentrations in space and time. This is due to the fact that atmospheric residence times of particles are shorter than mixing times within each hemisphere, and these are still shorter than mixing times between hemispheres. As a consequence, measurements made at any given time and place are not necessarily typical for other times and locations. Satellites that could provide adequate global and temporal coverages currently have too limited a capability for delineating relevant aerosol characteristics, and aircraft and ground measurements are too spotty in space and time to adequately determine the global distribution of aerosols. Moreover, aerosols cover several orders of magnitude in concentration (from less than one to several million per cubic centimeter) and size (from units of Ångströms for molecular clusters to millimeters for precipitation particles). No single instrument or technique has the capability to adequately assess atmospheric aerosol properties over this large a size range. Also, in contrast with trace gases, the concentration of aerosol particles is so sparse that measurements have significant experimental and statistical uncertainties.

What follows is an overview of (1) formation, evolution, transformation, and fate, (2) effects on climate, and (3) role in heterogeneous chemistry, including polar stratospheric clouds of man-made particles and the natural atmospheric background aerosol.

5.2. FORMATION, TRANSFORMATION, REMOVAL

5.2.1. Primary and Secondary Aerosols

Aerosols are formed by two general mechanisms. These are the break-up of material and the agglomeration of molecules. Accordingly, atmospheric aerosols may be either primary or secondary. If primary they are due to direct emission of particulate material into the atmosphere from both anthropogenic (e.g., urban/industrial processes, land use practices) and natural (e.g., volcanism, wind-blown dust, sea-spray) activities. Secondary aerosols result from particle formation by gas reactions.

5.2.2. Meteorological Effects

The duration and rate of generation at the Earth's surface and the subsequent atmospheric dispersion and residence time of aerosols are critically dependent on

types of emissions, on terrain, and on the prevailing meteorology. In still air, aerosol fluxes from the surface into the boundary layer occur as long as a positive radiation balance exists. Exchange stops by the time a surface temperature inversion has formed, and particles settle back to the Earth's surface from the boundary layer when the radiation balance is negative, e.g., at dusk. This is one reason for strong diurnal and seasonal variabilities of tropospheric concentrations. Temperature inversions aloft frequently cause aerosol layers (gradients of aerosol abundances) to form. Temperature inversions near the surface, initiated by low ground temperatures due to, e.g., ocean currents from Antarctica, greatly enhance smog episodes in cities along the Pacific coast from Santiago de Chile to Los Angeles. Wind and its causes (atmospheric temperature and pressure gradients) are important factors in the generation of primary aerosols.

5.2.3. Emission Rates

5.2.3.1. *Man-Made Aerosols*

Man's utilization of natural resources requires changing the physical form of these resources. Common examples are pulverization of coal, rock crushing, and cement manufacturing. The resulting emissions of primary particles can cause a severe local nuisance unless they are properly controlled.

Specific anthropogenic aerosol emissions result from fuel consumption in stationary sources (steam-electrical, industrial, commercial, institutional, and residential), industrial process losses (iron and steel mills, copper, lead, and zinc smelters, acid-manufacturing plants, petrochemical works, pulp mills, grain mills, etc.), solid waste disposals (municipal and on-site incineration and open and conical burning), transportation (gasoline and diesel vehicles, railroads, shipping vessels, aircraft, and non-highway machinery), agricultural activities including burning, and miscellaneous (forest and structural fires, coal refuse burning, organic solvent evaporation, and gasoline marketing).

Two approaches have been used to estimate global pollution emissions. Either the US emission data are extrapolated to the world, or global emission assessments are based on energy consumption and/or fossil fuel combustion rates by various nations. Both approaches yield estimates that 93–95% of the industrial aerosol precursor gases—hydrocarbons (HCs), nitrogen dioxide (NO₂) and sulfur dioxide (SO₂)—originate in the northern hemisphere, of which SO₂ emissions are of prime interest to man-made aerosol formation (Bates et al., 1992). In comparison with SO₂, the H₂S emissions from chemical processing and sewage treatment are rather small. Extrapolating US emission data of direct particle production by source category and particle size worldwide, estimates of global emissions of total anthropogenic aerosols (primary and secondary) are 323–690 Tg year⁻¹, the majority of which are contributed by submicrometer particles of diameter less than 1 μm (SCEP, 1970; see Table 5.1).

Emissions from agricultural burning are the major source of gaseous and particulate pollutants in the southern hemisphere. A combination of field measurements and meteorological diffusion modelling yields emission factors of 8×10^{-3} (8 kg of particulates per 1000 kg of material burned). With estimates of $2\text{--}5 \text{ Mg ha}^{-1} \text{ year}^{-1}$ of burnable material and a burnable area of up to 18×10^8 ha in 44 countries in tropical Africa, 30 countries in Central America, 10 countries in South America, 19 countries in tropical Asia, and 16 countries and islands in Oceania, the total emission of particulate material from agricultural burning is $29\text{--}72 \text{ Tg year}^{-1}$ (Bach, 1976).

The principal *aerosols of sulfur* in the atmosphere, mainly oxidation products of SO_2 , are acidic (H_2SO_4 ; NH_4HSO_4) and neutral ($(\text{NH}_4)_2\text{SO}_4$) sulfates. The annual rate of SO_2 emissions has increased from 10 Tg year^{-1} in 1860 to 150 Tg year^{-1} in 1980 (World Resources, 1989). The sources of man-made SO_2 emissions are coal combustion (68%), petroleum combustion (16%), smelting (11%), and petroleum refining (5%) operations. The increase in these activities in industrial times led to an increase in tropospheric non-sea-salt (NSS) sulphate from 0.19 to 0.53 Tg in the northern hemisphere and from 0.16 to 0.23 Tg in the southern hemisphere (Langner et al., 1992). The 1990 Clean Air Act Amendments in the United States call for a reduction by 50% of sulfur emissions and considerable reductions in nitrogen dioxide emissions. European countries are also moving rapidly toward emission reductions (e.g., Iversen et al., 1991). To the extent that these reductions are accomplished through reduced fuel use, they will have the double benefit of less sulfate particle generation and slower build-up of carbon dioxide in the air. Opposing a reduction of SO_2 emissions from an effective control strategy in Europe and America, however, is the largely uncontrolled increase in emissions of sulfur due to industrialization in developing countries, notably China.

Nitrate aerosol originates primarily from NO and NO_2 . From the sulfate/nitrate ratio of about 5:1, determined from 24 h high-volume samples from 217 urban stations across the US, and similar atmospheric residence times of both ions, the man-made nitrate emissions are $14\text{--}40 \text{ Tg year}^{-1}$ (Ludwig et al., 1970).

Extrapolating US emission values, global man-made *gaseous hydrocarbon* (HC) emissions are on the order of $80\text{--}90 \text{ Tg year}^{-1}$, 31% of which have been classified as reactive, i.e., they can participate in photochemical reactions in the atmosphere to form aerosols. The major contribution to this total amount is from petroleum combustion processes, including petroleum evaporation and transfer losses (55%), incineration (30%), solvent usage (10%), and others (5%). Bach (1976) assumed that about 75% of the 1968 US emission rate of 29 Tg year^{-1} consisted of non-methane compounds. If the world HC emission rate were that of the US, and if one-third of that amount were converted to HC aerosols, then a global production rate of about 15 Tg year^{-1} of man-made HC aerosols of submicron size could be expected.

Another class of anthropogenic aerosol with significance to both climate and heterogeneous chemistry is that of *black carbon or soot*. Black carbon aerosol (BCA) is produced during the incomplete combustion of fuels. The two most important sources are fossil fuel combustion and biomass burning. One estimate (Penner et al., 1993) puts the global emissions of BCA at 24 Tg year^{-1} . Measurements show that atmospheric concentrations of BCA vary between 200 and 800 ng m^{-3} in rural regions of the northern hemisphere but decrease to between 5 and 20 ng m^{-3} over ocean areas. Only a few ng m^{-3} of BCA occur at the South Pole and in the upper troposphere, while only a fraction of an ng m^{-3} of BCA is present in the stratosphere. Assuming an average tropospheric BCA concentration of 10 ng m^{-3} and an average tropopause height of 10 km , the average lifetime of BCA in the troposphere is 0.42 years or 152 days. Stratospheric concentrations are commensurate with polar route emissions from the current subsonic commercial aircraft fleet of $1.9 \times 10^9 \text{ g year}^{-1}$ of BCA (Turco, 1992), based on a fuel consumption of $1.5 \times 10^{14} \text{ g year}^{-1}$ and an emission factor of 10^{-4} .

5.2.3.2. Natural Aerosols

However important anthropogenic emissions may be close to their source, they are nevertheless unmatched on a global basis with the break-up and emission of particles by natural means. Eolian forces generating particles at the Earth's surface and transporting them either over land (wind-blown dust) or from sea to land (sea-salt spray), and volcanic forces ejecting particles from the Earth into the atmosphere, are responsible for the bulk of the natural primary aerosol. Other aerosol substances that may be locally important are those from wildfires and wind-blown dust. Only negligible contributions result from meteoritic dust originating in space.

Empirical relationships between wind speed u (m s^{-1}) and mass M ($\mu\text{g m}^{-3}$) of suspended particles (Jaenicke, 1986) are

$$M = 4.3 \exp(0.16u) \quad (5.1)$$

with u between 1 and 21 m s^{-1} over land, and

$$M = 52.8 \exp(0.30u) \quad (5.2)$$

with u between 0.5 and 18 m s^{-1} over water. Thus it follows that *wind-blown dust* is nature's major contribution to the primary continental aerosol. Soil material transported from arid regions by wind is responsible for the distribution of certain clay materials in oceanic sediments, and Saharan dust has a significant impact on the aerosol chemistry over the tropical North Atlantic. Estimates of global input from wind-blown dust range from 100 to 500 Tg year^{-1} . These are occasionally

influenced by man. For example, dust storms over America's Great Plains are related to agricultural activities, and Africa's Sahel has been rendered vulnerable to wind erosion by cattle overgrazing. The Great Plains are subject annually to occurrences of 45 h of dust stemming from dust storms of an average duration of 6 h, yielding dust concentration up to $5000 \mu\text{g m}^{-3}$. Dust loadings of $300\text{--}800 \mu\text{g m}^{-3}$ are found regularly in the lowest 5–10 km of the atmosphere over the Rajputana desert between India and Pakistan. Storms over the deserts and loess terrains of China and Mongolia produce dust that can be traced by satellites over distances of several thousand kilometers. Residues of Saharan dust amounting to average concentrations of $61 \mu\text{g m}^{-3}$ at 1.5–3.0 km altitude have been measured thousands of kilometers from their source over Barbados (Prospero and Carlson, 1972).

Primary *marine aerosols* result from the injection of sea-salt into the atmosphere. Estimates of the mass of airborne *sea-salt particles* at sea vary between 10 and $20 \mu\text{g m}^{-3}$ (Prospero and Carlson, 1972). Assuming that the majority of sea-salt is dispersed within the planetary boundary layer 1000 m deep, the global concentration amounts to about 11 Tg. With a production rate of 1000Tg year^{-1} (Erickson, 1959), the resulting average residence time is 1.1×10^{-2} years or 4 days. Thus about 90% of marine aerosols settle out over the oceans. The remainder of 100Tg year^{-1} is carried across the ocean shores into continental air. Once over land, the concentration of sea-salt particles decreases rapidly to about 15% at 4 km and to about 8% at 30 km inland.

The frequency and intensity of *volcanic eruptions* (Lang, 1974) and estimations of the height of the eruption clouds and amounts of ejected material yield estimates of aerosol emissions due to volcanism between 25 and 550Tg year^{-1} . Most of the volcanic material is injected into the stratosphere. In contrast, the estimates of terrestrial accretion of *particles of extraterrestrial origin* fluctuate between 0.02 and 10Tg year^{-1} . Forest fires have been estimated to contribute between 3 and 150Tg year^{-1} of particulate material into the atmosphere.

The majority of secondary natural aerosols (those formed from gases) result from oxidation of sulfur gas emissions from land and sea. These source gases include H_2S , DMS, methanethiol, carbon disulfide (CS_2), carbonyl sulfide (COS), methyl mercaptans, and others. Reactions in the atmosphere of hydroxyl radicals (OH) with these sulfur compounds form sulfur dioxide (SO_2), which is a precursor gas that can be further oxidized to form sulfate aerosol particles. From tropospheric measurements of CS_2 and the rate constant for its conversion to COS, Turco et al. (1980) estimate that 5 Tg of OCS per year could be generated from CS_2 in the atmosphere. In addition, there are direct sources of OCS which include the refining and combustion of fossil fuels (1Tg year^{-1}), natural and agricultural fires ($0.2\text{--}0.3 \text{Tg year}^{-1}$), and soils (0.5Tg year^{-1}), yielding a total influx of from 1 to 10Tg year^{-1} , up to 50% of which may be anthropogenic.

The principal sources for natural H_2S are sulfate respiration and the decomposition of amino acids containing various thiol groups. Most natural sulfur gas on land (62 Tg year^{-1}) is produced from decaying vegetation and animals. In the marine environment most volatile sulfur is emitted in the form of dimethylsulfide (DMS) which is excreted by living planktonic algae (see Chapter 8 for more details). The only significant non-biological natural S flux is the emission of SO_2 and H_2S by volcanoes and fumaroles. This process releases on the order of 26 Tg year^{-1} , or about 10–20% of the total natural flux of gaseous sulfur to the atmosphere, of which 4 Tg year^{-1} are from volcanic eruptions.

Naturally produced secondary nitrate aerosols result mostly from NO and amount to 75 Tg year^{-1} , 80% of which are submicron size. Global emissions of natural hydrocarbons from vegetation (mostly terpene compounds) and from the soil amount to about 150 Tg year^{-1} , of which approximately half are converted to aerosol, resulting in an annual emission rate of about 75 Tg year^{-1} .

5.2.3.3. A Comparison

Table 5.1 summarizes existing estimates of natural and man-made aerosol emissions and/or aerosol precursor gases. The wide range of emission estimates indicates a great difficulty in assembling global or regional budgets for atmospheric aerosol. This is due to a small magnitude of aerosol mass concentrations in air compared with trace gas concentrations, and the amounts processed through the atmospheric portion of the elemental cycles that are involved. The resulting chemical heterogeneity, in addition to large temporal and spatial variabilities, adds to the difficulty in assembling atmospheric aerosol budgets.

In spite of a wide range of emission estimates, Table 5.1 suggests that global aerosol production seems to be dominated by natural sources. However, because two-thirds of the Earth's surface is water, another major percentage is polar, which leaves only about 2.5% of the Earth's surface, mainly in the eastern US, Europe, Japan and parts of Australia and Asia, where anthropogenic aerosol production occurs. The natural production over this same area amounts to only a fraction of the man-made production. Anthropogenic SO_2 emissions to the atmosphere (primarily from fossil fuel combustion and metal smelting) have increased over the industrial period and now exceed natural emissions of sulfur-containing gases on a global basis. They completely blanket natural emissions in industrialized regions. Hence it is safe to conclude, on the basis of Table 5.1, that urban/industrial aerosols are dominated by anthropogenic material. Plumes of light-scattering aerosol extending from industrial regions to the marine atmosphere have, like wind-blown desert dust, been discerned in satellite measurements. Examples of man-induced deteriorating air quality are the permanently poor visibility of generally less than 10 km in almost any European country, and smog episodes in cities along the west coast of the Americas, with Los Angeles probably the best-known example.

TABLE 5.1 Estimates of Global Emissions of Aerosols

Source	Strength (Tg year ⁻¹)	
	Natural	Anthropogenic
Primary particle production		
Transportation		2
Stationary fuel sources		43
Fly ash from coal		36
Non-fossil fuels		8
Petroleum combustion		2
Industrial processes		56
Iron and steel industry		9
Incineration		4
Cement production		7
Solid waste disposal		2
Miscellaneous		16–29
Soot		24
Agricultural burning		29–72
Sea salt	300–2000	
Soil dust	100–500	
Volcanic particles	25–300	
Meteoritic debris	0–10	
Forest fire smoke	3–150	
<i>Subtotal</i>	428–2810	215–260
Secondary particle production		
Sulfates from SO ₂		70–220
Sulfates from H ₂ S	105–420	
Sulfates from DMS	16–32	
Sulfates from volcanoes	9	
Biomass burning		3
Nitrate from NO _x	75–700	23–40
Ammonium from NH ₃	269	
Carbonates from hydrocarbons	15–200	15–90
<i>Subtotal</i>	195–1220	108–350
<i>Total</i>	623–4030	323–610

Both the optically effective and cloud-nucleating fractions of the atmospheric aerosol in urban/industrial regions are frequently dominated by sulfate particles. Residence times of SO₂ and SO₄²⁻ in the troposphere are short (several days) compared with mixing times in the troposphere (several months within hemispheres; about a year between hemispheres). Therefore anthropogenic aerosols in general and man-made sulfates in particular are concentrated mainly

in industrial regions and areas downwind of them, largely in mid-latitudes. Concentrations of aerosol sulfate and cloud condensation nuclei within 1000 km or more downwind of regions of industrial emissions are an order of magnitude or more greater than those in remote regions (Schwartz, 1989). Because more than 90% of industrial SO_2 is emitted in the northern hemisphere (Bates et al., 1992), anthropogenic sulfate is confined largely to that hemisphere. Widespread distribution of anthropogenic sulfate in the northern hemisphere is evidenced by elevated concentrations of non-sea-salt sulfate in the aerosol, in higher acidic precipitation at remote sites in the northern hemisphere relative to those in the southern hemisphere, and by increases in concentrations of sulfate in northern hemisphere glacial ice over the past 100 years (Mayewski et al., 1990) that closely match the record of anthropogenic emissions. Mass concentrations of non-sea-salt sulfate appear to be enhanced by 30% or more over the natural background in much of the marine northern hemisphere (Schwartz, 1989).

Considering an energy demand proportional to the increase in the Earth's population, for which there is no limit in sight, it is clear that the man-made component of the atmospheric aerosol is going to increase, and inadvertent climate modification on scales large enough to affect habitability will have to be reckoned with (Kondratyev, 1986).

5.2.4. Transformation

While airborne, transformation of aerosol takes place owing to physical (coagulation between particles) and chemical (condensation of vapors and surface reactions) modifications. We have seen that agglomeration of gaseous molecules to form solid or liquid aerosols is an important mechanism of their formation. Further deposition of gases on airborne particles is a significant phenomenon of aerosol transformation.

5.2.4.1. Condensation

Interaction of water vapor, the most abundant gas in the atmosphere, with a fraction of the aerosol results in the development of clouds and fogs and is probably the most important process of particle transformation by agglomeration. Water vapor condenses preferentially on hygroscopic salt particles or on hygroscopic molecules such as SO_3 . As agglomeration proceeds, the particles grow, and non-spherical crystals become more spherical as water condenses on them. With the exception of a small class of hydrophobic aerosols, there is a continuous increase in the geometric mean diameter of sulfates and other salts at increasing ambient relative humidity (Blanchet and List, 1983). The change in size and/or shape and/or refractive index with increasing relative humidity results in an increase in the aerosol optical thickness in the visible and near-IR regions as long as the atmospheric water vapor partial pressure is greater than

approximately 5 mbar. There is little or no correlation between the spectral aerosol optical thickness and relative humidity when the relative humidity is in the low (0.45–0.75) range. A phase change from solid to liquid, or vice versa, at the point of deliquescence results in an abrupt change in size (and possibly shape) at a relative humidity that is typical for a given salt. It is thus possible to use the deliquescence temperature to classify a hygroscopic aerosol type, e.g., ammonium sulfate, and distinguish it from acidic sulfuric acid and ammonium bisulfate (Butcher and Charlson, 1972).

Particles with the greatest affinity for water act as CCNs, i.e., centers around which cloud drops can develop when the air is near saturation with respect to water (Köhler, 1926). The chemical composition of condensation nuclei is important for the process of cloud droplet formation (Pruppacher and Klett, 1978). The effect of different soluble compounds, e.g., NaCl and $(\text{NH}_4)_2\text{SO}_4$, on the hygroscopic growth and nucleation process is less important than is the difference between soluble and non-soluble material. Thus nucleation is a scavenging process that assists in preferential precipitation of the more hygroscopic species of aerosols. Less hygroscopic or even hydrophobic species remain in the cloud and may be transported farther in the atmosphere after the cloud has dissipated. The more hygroscopic a CCN, the earlier it will become a droplet as water saturation is approached. At a given composition, larger CCNs will acquire water first. Consequently, the larger droplets have nucleated on the larger aerosol particles (Twohy et al., 1989). If the saturation increases further, smaller droplets become activated and dilute more quickly than the larger droplets because of their larger ratio of surface area to volume. Because sulfates are generally smaller than sea-salt particles, the size-selective nucleation process will result in the sulfate-dominated particles growing into smaller cloud droplets and the supermicrometer, e.g., sea-salt and soil dust, particles becoming the larger droplets. Soil dust and soot particles, although initially hydrophobic, can be made hygroscopic while airborne through the acquisition of SO_4^{2-} and other salts by coagulation.

The process of cloud formation was first explained on thermodynamical grounds by Köhler (1926). Figure 5.1 shows the calculated saturation ratio (expressed as relative humidity) versus particle size for one particular salt. At very low humidities the hygroscopic aerosol (salt) particle is dry and crystalline. Increasing the relative humidity initially causes some water to be adsorbed on the particle surface, but the amount is insufficient to dissolve the salt and the particle remains largely crystalline. Hence the growth in particle size is small. At a certain critical relative humidity, which is typical for the type of salt particle, the crystal takes up enough water to form a saturated solution. At this point the size of the particle increases abruptly by a factor of 2–3. At higher relative humidities the increase in size follows a growth equation based on a combination of Raoult's law and the Kelvin relation for the dependence of the vapor pressure of a particle

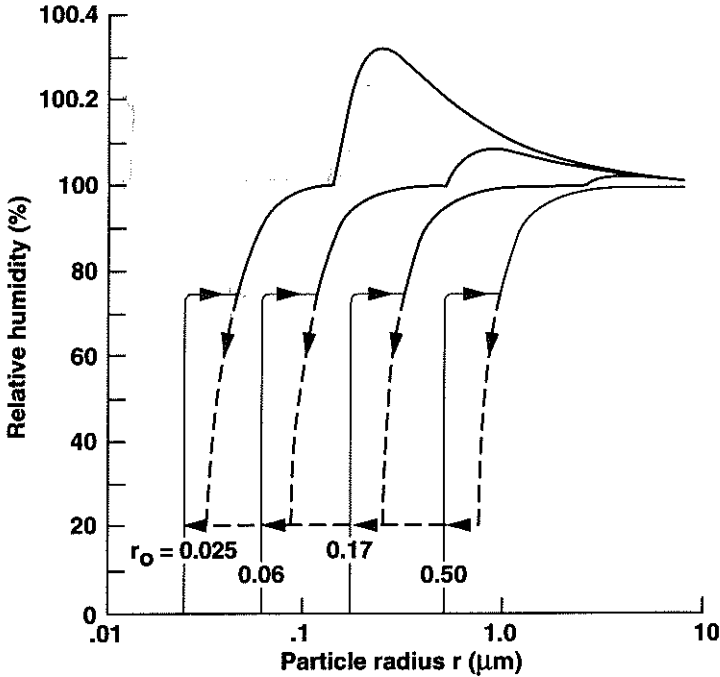


FIGURE 5.1. Köhler diagram: variation in particle size with relative humidity p/p_s , for a salt deliquescing at $p/p_s = 0.75$ (typical for NaCl) for CCNs of various sizes. (After Butcher and Charlson, 1972.)

on its radius. For a particle in equilibrium with its environment, the ratio of the actual vapor pressure of the solution droplet, p , to the saturated vapor pressure of water, p_s , is

$$\frac{p}{p_s} = \exp\left(\frac{2\sigma V}{RT r}\right) \left(1 + \frac{i m M_w}{M_s \left(\frac{4}{3}\pi r^3 \rho - m\right)}\right)^{-1} \quad (5.3)$$

where σ is the surface tension of a solution droplet, V is the molar volume of the liquid phase, T is the temperature, r is the droplet radius, i is the van't Hoff factor, i.e., the average number of moles of dissolved species produced per mole of solute, m is the mass of solute in the droplet, M_s is the molecular weight of solute, ρ is the density of a droplet, and M_w is the molecular weight of water. The validity of particle growth as a function of relative humidity has been tested and confirmed experimentally (Tang et al., 1977).

An important feature displayed by each growth curve in Figure 5.1 is the maximum in the domain of supersaturation above 100% relative humidity. It

indicates the degree of supersaturation required for a particle to form a stable cloud droplet. Once a particle has grown just beyond the maximum, it enters a region of instability and must grow further, provided that the water supply in the ambient air suffices.

Upon decreasing the relative humidity to values below the deliquescence point, the solution becomes supersaturated. Recrystallization does not occur as spontaneously as deliquescence, so that the particle size moves along the extended Köhler curve for a while before it shrinks to a value near the dry radius at low humidities ($< 20\%$). This hysteresis indicates an important mediation of aerosol size by clouds, with consequences for atmospheric optics and chemistry. Many cycles of cloud particle condensation and evaporation may take place long prior to the formation of precipitable particles, affecting the size and elemental composition of aerosols. Thus a cloud upon evaporation leaves behind an "activated" aerosol particle of a size that is larger than was the CCN upon which the droplet had initially formed. The larger surface area renders the particle more active both optically and chemically.

5.2.4.2. Oxidation and Neutralization

Next to condensation, important processes of particle transformation are oxidation and neutralization reactions on existing particles. In the cloudless atmosphere, gas phase oxidation of DMS, OCS, or CS_2 to SO_2 is proportional to the concentration of hydroxyl (OH), which varies substantially in space and time. It is most abundant in the boundary layer and in the upper troposphere during summer. Aqueous phase oxidation of SO_2 is proportional to cloudiness and, in winter, dominates in the lower and middle troposphere where clouds are abundant. Studies of the oxidation of SO_2 to SO_4^{2-} in the atmosphere indicate that condensed, aqueous phase reactions are important and can even be the main mechanism under atmospheric conditions when the aqueous phase is present in clouds, fogs, and high-humidity hazes. Thus, in a mixture of hygroscopic and hydrophobic particles, the oxidation of SO_2 will be favored in or on the former at high humidity.

Further reaction between OH and SO_2 results in the oxidation of SO_2 to SO_4^{2-} to form an H_2SO_4 aerosol. Acidic aerosols (H_2SO_4 and NH_4HSO_4) can be neutralized to $(\text{NH}_4)_2\text{SO}_4$ in the presence of ammonia vapor. Chemical reactivity of these water-soluble fractions is important with respect to various atmospheric and biogeochemical processes. Faster photochemical production of SO_4^{2-} from SO_2 gas-to-particle conversion takes place in summer, since the SO_2 and OH concentrations are higher in summer than in winter. The result is seasonal and diurnal variability in the physical and chemical properties of aerosol. Both aerosol number and volume concentrations and the SO_4^{2-} concentration are highest in the summer troposphere over the rural south-central United States.

5.2.4.3. Coagulation

Through Brownian motion, particles smaller than $1\ \mu\text{m}$ diameter continually migrate through the air and occasionally collide with other particles. A certain fraction of collisions will make the particles stick to one another, leaving them united to form a larger particle. This process causes a continual removal of small particles and an enhancement of larger ones. The rate at which this occurs depends upon the composition of the particles, the pressure-dependent velocity of their movements, the cross-sectional area of each particle and, most importantly, the particle concentration.

5.2.5. Removal

5.2.5.1. Dry Deposition

Diffusion and sedimentation are processes by which particles are brought into contact with the Earth's surface. Aerosol particles may migrate in and out of a control volume either by their own thermal agitation (Brownian motion) or by turbulent eddying of air. Brownian diffusivity in the atmosphere is exceedingly small ($10^{-8} < D < 10^{-4}\ \text{cm}^2\ \text{s}^{-1}$) for realistic particles sizes ($0.01 < r < 10\ \mu\text{m}$) compared with turbulent eddy diffusivity D_T for mass transport ($10^2 < D_T < 10^5\ \text{cm}^2\ \text{s}^{-1}$). The magnitude of diffusivity depends on the proximity to the ground and on conditions of local hydrostatic stability of the air. In general, turbulent diffusion will exceed the effect of Brownian motion for atmospheric transport, except in very thin layers near surfaces such as leaves or stones, where the air motion will be slow and laminar in nature.

The transfer of gases or aerosol particles from turbulent air to an underlying boundary depends on the properties of the flow near the surface as well as on the nature of the surface itself. In a simplified picture, transfer takes place through a turbulent boundary layer into a viscous or laminar sublayer adjacent to the boundary. The boundary layers are identified with a velocity gradient and with a gradient in concentration of diffusing aerosols. In the turbulent layer these gradients will be essentially similar in thickness because of the dominance of the eddying motion of the turbulence. In contrast, in the viscous sublayer, defined by gradients of properties, the nature of the transfer mechanism will depend primarily on molecular properties of the air. Its thickness will then vary with the molecular diffusivity of the species being transferred. Since molecular transfer is quite slow compared with that in the turbulent layer, the mechanism of transport in the sublayer is the rate-limiting mechanism of the process, and deposition of aerosols on surfaces will vary with the molecular (or Brownian) diffusivity as indicated in Figure 5.2, which shows the deposition velocity as a function of particle diffusivity and particle size for flow over smooth boundaries.

In the absence of horizontal concentration gradients the loss rate per unit volume for diffusional transport is given as

$$L_D = -D_T \delta^2 n / \delta Z^2 \tag{5.4}$$

As particles increase in size, first through their formation by the agglomeration of molecules in condensing vapors and later by the coagulation of pairs of particles, the effect of gravity may become more important than that of Brownian motion. Sedimentation then becomes a factor which removes aerosols from the air. In a dry, still atmosphere the upper limit for aerosol sizes is determined by sedimentation. The gravitational force experienced by a particle is $f_g = mg$, where m is the mass of the particle and g is the acceleration due to gravity. Once the particle has acquired a downward velocity, it will experience an opposing force $f_d = 6\pi\eta r v$ due to the friction with air, where η is the viscosity of air, r is the particle radius, and v is its velocity. Equating these two forces results in a settling velocity of particles

$$v_s = 2r^2 \rho g / 9\eta \tag{5.5}$$

with which a particle of a given size will approach the ground. The deposition velocity for particles settling out at the surface is identical with the sedimentation velocity. Thus the rate of sedimentation increases rapidly with particle size. Other factors influencing settling rates, albeit less importantly than does particle size, are particle shape and particle density. The deposition flux F_d can be estimated by

$$F_d = v_s \delta n / \delta Z \tag{5.6}$$

where $\delta n / \delta Z$ is the concentration gradient of particles with altitude.

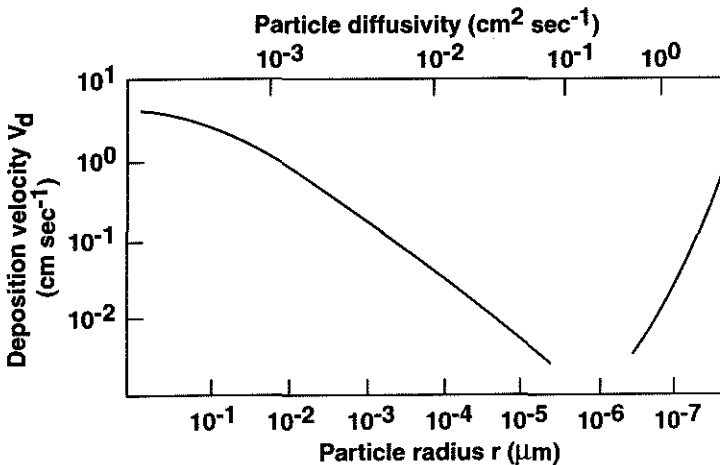


FIGURE 5.2. Deposition velocity as function of particle size. (After Hidy, 1973.)

Dry deposition of aerosol is thus proportional to its surface concentration. Its removal rate is determined by the deposition velocity, the vertical turbulent diffusion coefficient of the boundary layer, and the vertical distance between the surface and the height at which the aerosol occurs.

5.2.5.2. Wet Removal

In addition to removal by dry deposition, removal of aerosols near the surface takes place by precipitation, preceded by in-cloud and subcloud scavenging. The estimation of the loss of particles by rain-out involves complicated and interacting factors that may contribute to scavenging of aerosols by cloud droplets and ice crystals. One mechanism for trapping particles is nucleation of the hydrometeor (see Section 5.2.4). Others involve migration of the particles to the cloud drop by (a) thermophoretic forces during condensation or evaporation, (b) electrical interactions, or (c) thermal agitation. The amount of aerosol removed from air by cloud formation can be approximated by

$$\Delta n = E_n n_a \quad (5.7)$$

where E_n is a cloud scavenging efficiency that involves many factors (solubility, particle size, etc.) and n_a is the particle concentration in air. Δn must be proportional to the amount of water vapor ingested by the cloud during formation. The amount of water vapor removed from the air during cloud formation can be approximated as

$$\Delta q = q_a - q_s(T_c) \quad (5.8)$$

where q_a is the water vapor content of air and $q_s(T_c)$ is the corresponding saturated humidity of air at cloud temperature T_c . The scavenging ratio $R = n_c/n_a$, where n_c is the aerosol concentration in cloud droplets, can be expressed as

$$R = \frac{\Delta n/\Delta q}{n_a} = \frac{E_n}{q_a - q_s(T_c)} \quad (5.9)$$

In-cloud scavenging of particles (Junge and Gustafson, 1957) is dependent on the average rate of formation of precipitation and the liquid water content of the rain cloud. Empirical relationships show an efficiency of wet removal that is approximately 10% of the liquid water content. Typical values of liquid water content are $1\text{--}2\text{ g m}^{-3}$ for precipitating clouds and $0.05\text{--}0.25\text{ g m}^{-3}$ for convective and stratiform clouds (Mason, 1971). Wet removal efficiencies E_n will therefore lie in the range $0.5\% < E_n < 20\%$.

Scavenging will also occur as the larger cloud particles fall downward. If the falling hydrometeors are evaporating, a temperature gradient could develop

between them and the surrounding air, such that thermophoresis may have to be considered. Scavenging of particles by hydrometeors falling from clouds located above the aerosol and isolated from it by stratification will eventually cleanse the entire underlying air layer and dissolve its contents in the total quantity of deposited water if the precipitation event lasts long enough. Hence in the limit an inverse relationship between concentration in precipitation and amount of precipitation would result. The process involved is analog to that of radioactive decay, where it is commonly assumed that the rate of removal at any instant is proportional to the quantity of radioactive material. Therefore at any instant of a precipitation event the rate of change with time in particle concentration can be written as

$$\Delta n_a / \Delta t = -\lambda n_a \quad (5.10)$$

where λ is a scavenging rate. Empirical data show $0.5 \times 10^{-5} < \lambda < 15 \times 10^{-5}$ for stratiform systems and $5 \times 10^{-5} < \lambda < 3 \times 10^{-3}$ for convective systems (Hicks, 1986). Integration leads to

$$n_a(t) = n_{a0} \exp(-\lambda t) \quad (5.11)$$

where $n_a(t)$ is the concentration as function of time and n_{a0} is the concentration at the onset of precipitation at $t = 0$.

If uniformly mixed throughout a layer of the atmosphere of depth h , the total quantity removed in an event of duration t is obtained by integration as

$$h(n_{a0} - n_{at}) = hn_{a0}[1 - \exp(-\lambda t)] \quad (5.12)$$

If rainfall rate is I and $p (= It)$ is total precipitation, then the concentration in the precipitation falling in the course of an event is

$$n_p = \frac{hn_{a0}[1 - \exp(-\lambda t)]}{It}$$

$$n_p = \frac{hn_{a0}[1 - \exp(-\lambda p/I)]}{p}$$

$$R = n_p/n_{at} = \frac{h \exp(1 - \lambda_p/I)}{p} \quad (5.13)$$

In this derivation of R it is assumed that λ is constant, which is a simplification. In reality, λ is expected to vary with particle size, particle solubility, precipitation rate, etc.

The best quantitative information on the deposition (dry and wet) fluxes of NSS sulfate comes from ice core records obtained in Greenland, showing an enhancement by a factor of 2–4 over the last hundred years (Neftel et al., 1985). This agrees well with calculated changes of 2–5 in total NSS sulfate by Langner et al. (1992) over 58% of the northern and over 16% of the southern hemisphere surface area.

5.2.6. Residence Times

The rates of formation, agglomeration, coagulation, and removal, in combination with a size-dependent water solubility of particles, determines the atmospheric residence times of aerosols. They can be described by an empirical equation (Jaenicke, 1986)

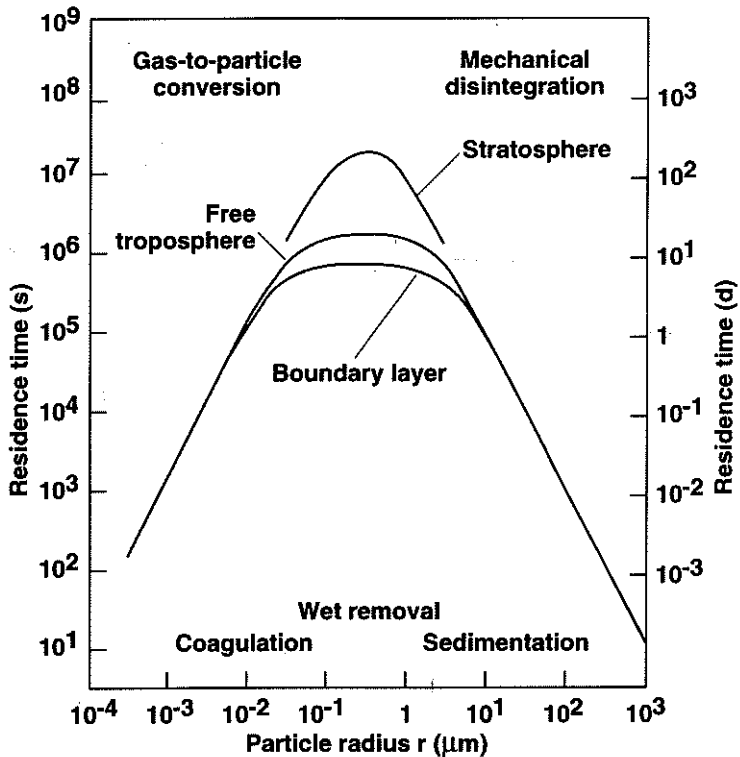


FIGURE 5.3. Atmospheric residence times as function of particle size. (After Jaenicke, 1986.)

$$\frac{1}{\tau} = \frac{r^2}{FR^2} + \frac{R^2}{Kr^2} + \frac{1}{\tau_{\text{wet}}} \quad (5.14)$$

where τ is the residence time, τ_{wet} is the wet removal residence time, K and F are constants, and $r = 0.3 \mu\text{m}$ is the radius of particles whose residence time is the longest.

Figure 5.3 is a graphical depiction of residence time as function of particle size. It shows that the residence for small and large particles is relatively short. Small particles are subject to Brownian motion, resulting in a high rate of coagulation. The large particles have settling velocities of several cm s^{-1} , resulting in a fairly high rate of sedimentation. Residence time is largest in the stratosphere. This is due to the fact that volcanic eruptions, the major source of stratospheric particles and their precursors, are rather sparse. In addition, the absence of water vapor in significant amounts in the stratosphere prevents cloud formation which renders wet removal ineffective. Such source and sink limitations let coagulation and sedimentation proceed very effectively to produce the surface area distribution shown as a dashed curve in Figure 5.6 (see Section 5.3).

5.2.7. Size Distributions

With the process of coagulation determining the lower end of the size spectrum, and that of removal the upper end, the question arises whether a unique size distribution of particles in the atmosphere can be established which, according to Friedlander (1970), should be called the “self-preserving” distribution.

Studies of atmospheric aerosol have shown that there are generally three peaks within the particle size range between 0.01 and $10 \mu\text{m}$, dubbed by Whitby (1978) the nucleation, the accumulation, and the coarse particle modes. Figure 5.4 summarizes the formation, transformation, and removal processes (after Whitby, 1978). It is a schematic of the distribution of aerosol surface area with particle size, showing the three major modes, the main source of mass for each mode, the principle processes involved in inserting mass into each mode, and the principle removal mechanisms. The nucleation and coarse particle modes are prevalent near the sources of particles. As an aerosol evolves with time away from sources, the dominant mode is the accumulation mode around $0.1 \mu\text{m}$ diameter. Figure 5.5 gives an example of a particle size distribution that is frequently observed in the free troposphere.

A striking feature of atmospheric aerosols is a steady decrease in particle number per unit volume of particles above $0.1 \mu\text{m}$ size, which prompted Junge (1961) to point out first that the distribution of particles larger than $0.1 \mu\text{m}$ can often be approximated by a power law

$$\frac{\Delta n(r)}{\Delta r} = Cr^{-(\beta + 1)} \quad (5.15)$$

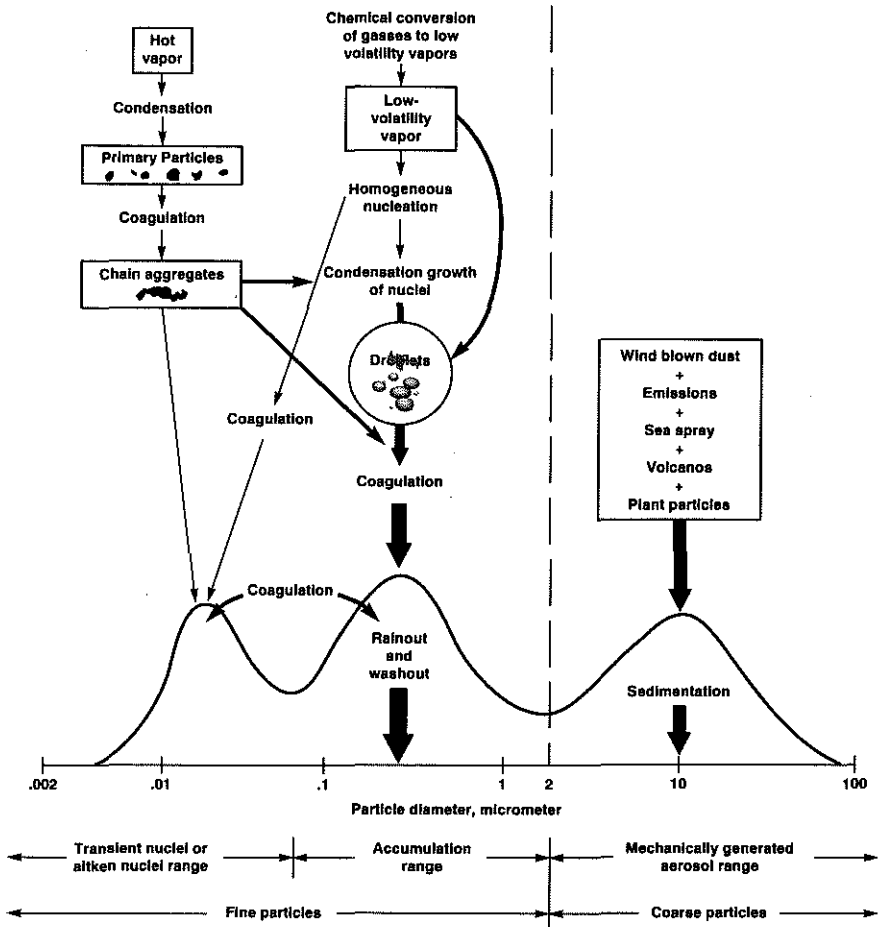


FIGURE 5.4. Schematic of an atmospheric aerosol surface area distribution showing the three modes, the major sources for and principal processes involved in inserting mass into each mode, and the principal removal mechanisms. (After Whitby, 1978.)

where Δn is the concentration of particles whose radius r lies between r and $r + \Delta r$, and C is a constant. The value of β usually averages 3, although variations between 2.5 and 4 are not uncommon, depending upon the type of aerosol and its atmospheric residence time. The power law distribution is a special case of a log-normal distribution

$$\frac{\Delta n(r)}{\Delta r} = \frac{n_o}{r \ln \sigma_g \sqrt{2\pi}} \exp \left[-\frac{1}{2} \left(\frac{\ln r - \ln r_g}{\ln \sigma_g} \right)^2 \right] \quad (5.16)$$

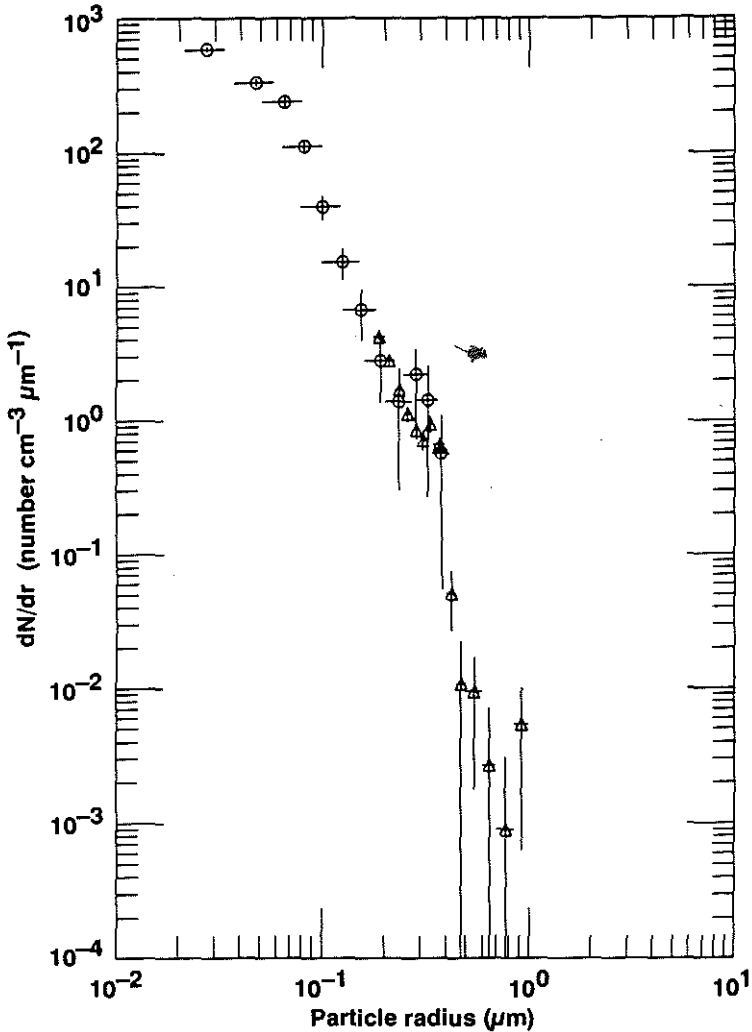


FIGURE 5.5. Aerosol size distribution measured in the free troposphere by impactors (circles) and optical particle counters (triangles). (After Pueschel et al., 1994a.)

which more universally describes each particle mode by the concentration per unit volume, n_0 , the geometric mean radius r_g , and the geometric standard deviation σ_g . The great range of particle sizes, with the ratio between the extreme sizes often on the order 100:1 or greater, renders the log-normal distribution a suitable tool for describing the distribution of particle sizes. According to the log-

normal distribution law, one of the most important in nature, it is the logarithm of particle size that is normally distributed.

5.2.8. Composition

The composition of the aerosol depends upon the sources and subsequent transformation while airborne. In a first approximation it is thus possible to distinguish continental from maritime aerosols, although mixing between the two types is often the case. The composition of continental aerosols, furthermore, varies from urban to rural areas, determined by the local types of natural and anthropogenic sources and the distance from these sources. In general, the aerosol represents a mixture of substances from various sources, and any specific component may have more than one origin.

Sulfate is the dominant inorganic constituent of aerosols, except for the marine aerosol which is dominated by sodium chloride (NaCl). SO_4^{2-} mass fractions range from 22% for continental aerosols to 75% in the Arctic and Antarctic regions. The origin of sulfates over the continent is SO_2 gas-to-particle conversion, because (1) the sulfur content of the Earth's crust is too low to provide a significant source of primary sulfates and (2) sulfate is concentrated in particles of submicron size.

Near sources of gaseous ammonia, NH_4^+ is the principal cation associated with sulfate in the continental aerosol. The degree of neutralization of sulfuric acid in parts of the troposphere depends on the supply of NH_3 relative to the rate of formation of H_2SO_4 . Molar $\text{NH}_4^+/\text{SO}_4^{2-}$ ratios range from 1 to 2, suggesting a composition intermediate between NH_4HSO_4 and $(\text{NH}_4)_2\text{SO}_4$. Over much of the oceans, in the continental remote troposphere, and in the stratosphere the major aerosol component is H_2SO_4 . As was pointed out earlier, sulfate in the aerosol shows seasonal variability. The mid-latitude sulfate aerosol concentration is highest in summer owing to both higher SO_2 emission rates and greater OH concentrations. The Arctic aerosol, in contrast, has a high SO_4^{2-} content in winter.

Long-range transport of anthropogenic aerosol results in modifications of the atmosphere long distances away from the particle sources. Polar regions are sinks for most atmospheric trace constituents, including aerosols. Once introduced into the Arctic atmosphere, a combination of different source regions, thermal atmospheric stability, reduced photochemistry, low scavenging rates, and slow meridional transport produces a complex, vertically layered atmosphere in which very clean and quite polluted air can alternate and can potentially last for a long time. Early airborne observations made it clear that the particulate portion of this pollution contributed to a significant degradation of visibilities to as low as 3–8 km. These episodes of anthropogenic pollution (haze events) are also common at surface locations around the Arctic rim in winter. The haze contains secondary aerosol (mostly acidic sulfates) and primary aerosol of industrial

origins, mixed with natural aerosols made up of soil and volcanic material. Concentrations in winter are typically one magnitude higher than in summer throughout most of the Arctic troposphere. The covariation in SO_4^{2-} with vanadium, which is partly a product of fossil fuel combustion, and with the concentrations of radon and its decay product ^{210}Pb , as well as air mass trajectory analyses, suggests that Arctic air pollutants originate at mid-latitudes, mainly in Europe, and are transported to the Arctic via Russia.

In contrast, a natural source of the SO_4^{2-} content, similar in abundance to that in the Arctic, must be invoked for the Antarctic aerosol because of the absence of anthropogenic pollution in this region. The fine and coarse aerosol particle composition in the Antarctic atmosphere shows sulfur preferentially as CaSO_4 or NH_4HSO_4 for particles in the size range $0.1\text{--}2.0\ \mu\text{m}$, with a higher CaSO_4 particle concentration in summer. Other types of particles are NaCl and MgCl_2 from sea-salt. A large number of these show small (1%) amounts of sulfur, indicating reactions of these particles with gaseous sulfur.

Sulfate in the marine aerosol is present in both the accumulation and coarse particle modes, indicating that its ionic composition is quantitatively different from that of the continental aerosol, where SO_4^{2-} is found mainly in the accumulation mode. The coarse particle fraction is associated with sea-spray, whereas the submicrometer-size fraction again results from SO_2 gas-to-particle conversion. The major gaseous precursor of sulfate in the unperturbed marine atmosphere is dimethyl sulfide, a biogenic compound emanating from the sea surface. Oxidation pathways for dimethyl sulfide are discussed in Chapter 8. The main anions of the marine aerosol are Na, Cl, Mg, K, and Ca, which make up the coarse particle mode.

Particulate nitrate in the marine aerosol is associated mainly with coarse particles. Its source must be gaseous nitric acid, because sea-water contains insignificant amounts of nitrate. That gaseous nitrate condenses preferentially onto coarse particles, in contrast with sulfate, has to do with its volatility, which is much higher than that of sulfuric acid, thus preventing simultaneous condensation in the same size range. The association of nitrate with the bulk of sea-salt may also result from the dissolution of nitric acid in the sea-water droplets at relative humidities in excess of 75%. In the continental aerosol, nitrate is distributed over the whole $0.1\text{--}10\ \mu\text{m}$ size range. In coarse particles it is mainly balanced by sodium, and in the submicrometer particles by ammonium.

Some trace components of the aerosol are considerably enriched compared with their abundances in the Earth's crust and in the oceans. The enrichment factor EF is defined as

$$\text{EF}(\text{X}) = \frac{\text{F}(\text{X})/(\text{Ref})_{\text{aerosol}}}{(\text{X})/(\text{Ref})_{\text{source}}} \quad (5.17)$$

where X is the element under consideration and Ref is an appropriate reference element. Useful reference elements are Al for crustal materials and Na for seawater.

There is sometimes a marked difference in the composition of aerosols in cities dominated by sulfurous smog and those with photochemical smog. In the latter there is a considerably higher concentration of organic aerosols and nitrates, and very often a lower concentration of sulfates. In a city such as Los Angeles, probably 20–40% of the aerosols are primary pollutants and 30% are secondary. The remainder appears to be representative of the natural background concentration. In cities with sulfurous smog, much of the aerosol matter is ash or waste from chemical processes. Table 5.2 summarizes what is known about the chemical composition of the three major atmospheric aerosol types.

TABLE 5.2 Mass Concentrations ($\mu\text{g m}^{-3}$) of Components in Three Aerosol Types

Element or Compound	Urban Aerosol		Continental	Marine
	Sulfurous Smog	Photochemical Smog		
SO_4^{2-}	14.0	16.5	0.5–5	2.6
NO_3^-	3	10	0.4–1.4	0.05
Cl^-	3.2	0.7	0.08–0.14	4.6
Br^-	0.1	0.5	–	0.02
NH_4^+	4.8	6.90	0.4–2.0	0.16
Na^+	1.2	3.1	0.02–0.08	2.9
K^+	0.4	0.9	0.03–0.1	0.1
Ca^{2+}	1.6	1.9	0.04–0.3	0.2
Mg^{2+}	0.6	1.4	–	0.4
Al_2O_3	3.6	6.4	0.08–0.4	–
SiO_2	5.9	21.1	0.2–1.3	–
Fe_2O_3	5.3	3.8	0.04–0.4	0.07
CaO	–	–	0.06–0.18	–
Organics	27.1	30.4	1.1	0.9
<i>Sum</i>	43.5	75.7	1.8–11.0	11.2

Selected mass fractions, molar and elemental ratios

SO_4^{2-} (%)	29.5	21.8	30.2–45.7	22.6
NO_3^- (%)	6.3	12.8	13.3–22.7	0.44
$\text{NH}_4^+/\text{SO}_4^{2-}$	1.9	2.2	2.1–3.4	0.47
Si/Al	1.4	2.9	1.9–2.8	–
Fe/Al	1.9	0.8	0.6–1.2	–
Na/Al	0.6	0.9	0.4–0.6	–
K/Al	0.2	0.3	0.5–0.6	–
Ca/Al	0.8	0.6	1.9–2.1	–

5.2.9. Spatial Distributions

In the boundary layer, size distributions of the optically important 0.1–23.5 μm diameter range are typically bimodal with modes around 0.1 μm and several microns diameter, which are typical modal radii for the accumulation and coarse particle modes, respectively. The coarse mode decreases rapidly with increasing altitude owing to preferential settling and interactions with clouds. The relatively long-lived accumulation mode, of greater importance to long-range transport of sulfur pollutants, shows both horizontal and vertical variabilities. While horizontal homogeneity of aerosol concentrations over tens to hundreds of kilometers has been observed, vertically the accumulation mode forms layers. Typically there is a boundary layer aerosol mass concentration of 10–20 $\mu\text{g m}^{-3}$ below 900 mbar, then a band between 700 and 900 mbar with 2–5 $\mu\text{g m}^{-3}$, and a layer above 700 mbar that contains less than 2 $\mu\text{g m}^{-3}$ of particles. Finer vertical structures within each of these layers are frequently observed. The accumulation mode concentration off the Virginia coast can be twice that of Bermuda. At Bermuda the particulate burden reaching the islands from the west is enhanced by about 50% over the fluxes of background aerosol from the south and/or east.

Size distribution and composition of lower tropospheric aerosols are strongly influenced by prevailing meteorology. For example, sulfur-rich stratified aerosol layers are a common feature from 0 to 3000 m off the northeast American coastline. These occur under clear air conditions with airflow from west to east, but change dramatically during the encroachment of warm frontal systems. This causes the sulfate content to decrease several-fold, and chloride to become the most common water-soluble anion in the lower 3000 m, probably owing to increased vertical mixing and dilution of pollutant aerosols. Thus the structure and stability of stratified atmospheric layers are important in studies of the ocean-atmosphere chemistry problem.

5.3. STRATOSPHERIC AEROSOLS

A negative lapse rate above the tropopause, caused by absorption of solar radiation by ozone, results in a fairly dense aerosol layer, dubbed the Junge layer after its discoverer (Junge, 1961). Because of the high degree of stability of the stratosphere, there is little vertical convection. This and the absence of clouds due to a lack of moisture result in aerosol residence times of a year or more (compared with days in the troposphere). This distinction between stratospheric and tropospheric aerosols justifies a separate discussion of stratospheric aerosol.

During large volcanic eruptions, large amounts of gases in the form of sulfur dioxide and hydrogen sulfide, and large numbers of particles such as ash and

sulfates, are injected into the stratosphere. Relatively small but sulfur-rich volcanic eruptions can have atmospheric effects equal to or even greater than much larger sulfur-poor eruptions. Small eruptions are probably the most frequent source of stratospheric aerosols. Figure 5.6 shows an example of a stratospheric background (dashed curve) and a volcanically enhanced (solid curve) stratospheric aerosol size distribution.

During volcanic quiescence, the origin of the stratospheric aerosol is not exactly known. We know that there is a common source of sulfur compounds for the stratosphere in both the northern and southern hemispheres. The precursor gas of the stratospheric aerosol is SO_2 of mostly volcanic, but also possibly of biogenic or anthropogenic, origin. Carbonyl sulfide (OCS), an oxidation product of carbonyl disulfide (CS_2) with an atmospheric lifetime of about 1 year, is a candidate for stratospheric sulfur aerosols.

The sulfuric acid aerosol is formed by photochemical reaction of sulfur gases with water vapor in the stratosphere. Particle formation is strongly temperature-dependent. Extremely explosive eruptions may also inject amounts of chlorine into the stratosphere in the form of hydrogen chloride to induce chemical reactions that lead to ozone losses similar to those caused by chlorofluoromethanes (see Section 5.4.2). Particles are formed in the stratosphere from sulfur gases either by some sort of *in situ* homogeneous nucleation mechanism, including binary and ternary nucleation, or by binary heterogeneous nucleation onto particulates (i.e., condensation nuclei). These could be injected into the stratosphere from the troposphere or from outer space (such as with meteoritic debris or ion clusters). If homogeneous nucleation occurs, the formation of new particles involving H_2SO_4 - HNO_3 - H_2O ternary reactions may be the most favorable mechanism for the formation of stratospheric aerosols (Kiang et al., 1975). This is because vapor pressures for the ternary system H_2SO_4 - HNO_3 - H_2O (with weight composition around 70–80% H_2SO_4 , 10–29% HNO_3 , 10–20% H_2O) are at -50°C low enough to prevent evaporation. If this mechanism operates, acids of nitrogen should be present in stratospheric aerosols in addition to H_2O and H_2SO_4 . Indeed, Farlow et al. (1978) tentatively identified two forms of nitrosyl sulfuric acid (NOHSO_4 and NOHS_2O_7) in stratospheric aerosols. The first of these can be formed either directly from gas reactions of NO_2 with SO_2 , or by gas-particle interactions between NO_2 and H_2SO_4 . The second product may form when SO_3 is involved. Estimates based on these reactions suggest that the maximum quantity of NO that might be absorbed in stratospheric aerosols could vary from one-third to twice the amount of NO in the surrounding air. If these reactions occur in the stratosphere, then a mechanism exists for removing nitrogen oxides from that region by aerosol particle fall-out. This process may typify a natural means that helps cleanse the lower stratosphere of excessive pollutants and results in ozone depletion. Burley and Johnston (1992) revived

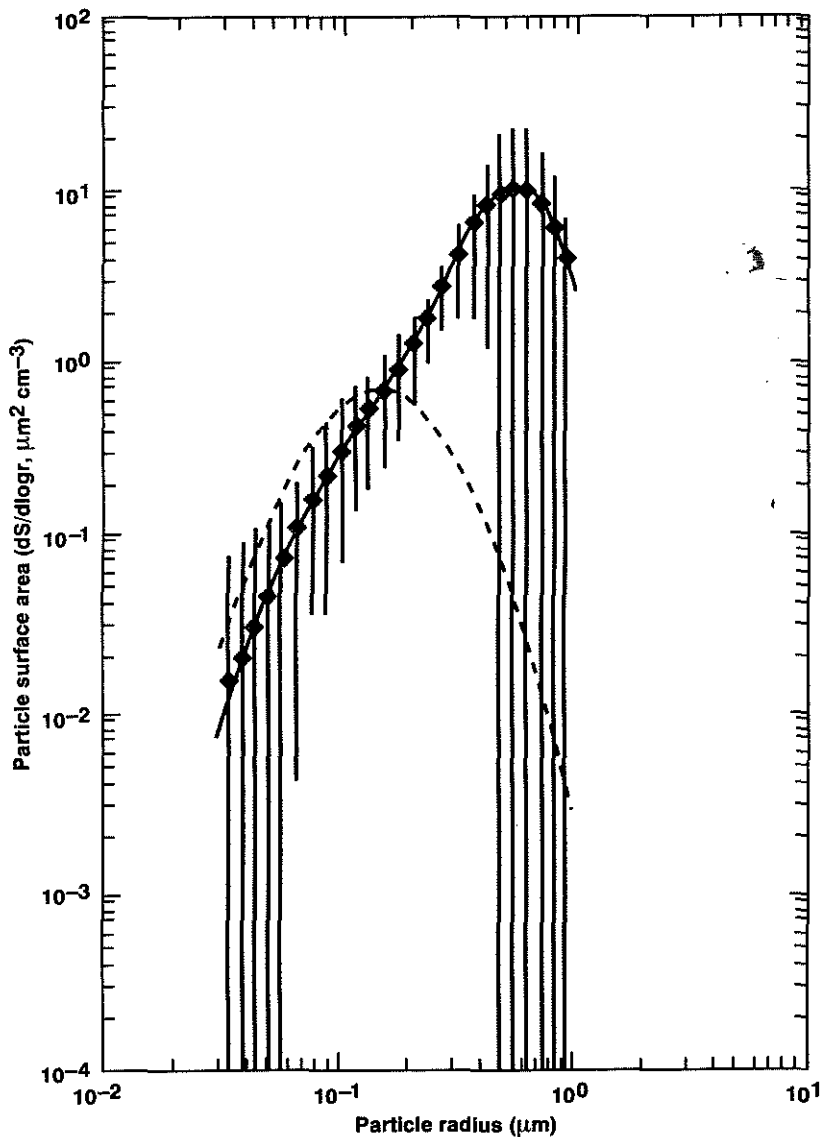


FIGURE 5.6. Mean and standard deviation of the surface area distribution of 28 samples of the Pinatubo volcanic aerosol collected between August 1991 and March 1992. The dashed curve represents the surface area distribution of a "background" sample collected over Antarctica in August 1987. (After Poeschel et al., 1994b.)

the nitrosyl sulfuric acid issue in connection with ozone depletion by heterogeneous reactions of NO_x with stratospheric aerosols (see Section 4.2).

Because of a strong temperature dependence of homogeneous nucleation rates (Yue and Deepak, 1982), the particles appear to be formed in polar regions during the cold winter and advected to lower latitudes. Since most of them do not seem to contain inclusions, it is believed that they are the product of homogeneous nucleation of sulfuric acid and water. The larger sulfuric acid aerosol particles, however, do sometimes contain some sort of insoluble inclusion (or at least some material remnant which survives evaporation). It is not certain whether this is an indication of a heterogeneous nucleation process or just the fact that these are aged aerosol particles which have undergone coagulation with available material.

In general, there is a tropical source for the reacting gases, a slow average transport to higher latitudes, and a formation of aerosol particles by growth onto the condensation nuclei (CNs) produced in the winter polar vortices. The sulfuric acid vapor which gives rise to the new particle formation in the winter polar vortices can also originate at mid-latitudes by evaporation of aerosols at high altitudes (above about 30 km the temperature is too high to support the aerosol and the particles evaporate) which leads to a supply of gas phase sulfuric acid which will migrate to the poles. During the winter descent of air, this sulfuric acid is carried to lower levels. Since the temperature is low enough, nucleation will occur. Since this air is relatively particle free, coagulation will not reduce the number density too quickly. With the breakdown of the polar vortex, these particles are advected to the mid-latitudes and serve to maintain the sulfate layer by supplying new particles.

With regard to the fate of stratospheric aerosols, it is believed that the particles near the bottom of the aerosol layer are removed by being mixed out into tropospheric air. The particles are probably mainly removed from the stratosphere at tropopause folds, which are a major sink for stratospheric air. Subsidence of air near the poles in winter may also account for a significant loss of stratospheric aerosol particles. Polar regions in the winter appear to be one of the most important sinks for stratospheric aerosols. Thus few if any of the particles injected into the stratosphere by the 1985 eruption of Redoubt volcano (60.5°N , 152.0°W) were observed in the tropics afterwards.

5.4. EFFECTS

5.4.1. Climatic Changes

Aerosol and cloud particles exert a variety of important influences on the Earth's climate and on the atmosphere's chemical composition and dynamics. An interplay between atmospheric, geophysical, solar, and geographic factors

influences the climatic effects of aerosols (Kondratyev, 1986). While population growth and growing industrialization may lead to unexpected (inadvertent) climatic changes, natural factors should predominate until the end of the century.

5.4.1.1. Direct Radiative Forcing

Natural aerosol constituents contribute to light scattering in the unperturbed atmosphere. These are submicron particles of sulfates and organic carbon (such as terpenes) produced by partial atmospheric oxidation of, respectively, gaseous biogenic sulfur and organic compounds. Sea salt and wind-blown dust can contribute locally, as can smoke and ash from volcanoes and wildfires. These sporadic events are globally less significant, however, because the particles are either generated too infrequently or they are large and short-lived, and thus transported only short distances.

The mid-visible optical thickness, a measure of the attenuation of sunlight in the free troposphere due to terpenes and sulfates, is $\tau \approx 0.01 \pm 0.005$ (Russell et al., 1993). With an average height of the tropopause of 15 km, the resulting extinction due to background aerosol scattering is about $7 \times 10^{-4} \text{ km}^{-1}$. This extinction value compares favorably with a computed light extinction based on *in situ* measured size distributions in the Pacific Basin free troposphere of about $2 \times 10^{-4} \text{ km}^{-1}$ (Pueschel et al., 1994a).

Critical for the direct climatic effects of anthropogenic sulfates is the amount of secondary aerosol formed from SO_2 emitted by fossil fuel combustion. About half the SO_2 is dry-deposited on the Earth's surface before oxidation to sulfates, and most of the remainder is oxidized in cloud droplets, such that only 6% of the sulfur emitted per year from anthropogenic activities is available for the gas phase production of new particles (Langner et al., 1992). However, because a cloud that may wet-oxidize SO_2 to produce H_2SO_4 goes through many cycles of condensation and evaporation before the droplets become large enough to precipitate out, cloud-oxidized sulfate particles can be released from an evaporating cloud and also participate in a direct forcing of climate. Therefore it appears that approximately 40–50% of the SO_2 emissions from the burning of fossil fuel are converted to new particles (Charlson et al., 1992).

The direct (non-cloud) radiative forcing by man-made sulfates has been estimated from empirical relations between light extinction and sulfate concentrations. Assume an annual emission of anthropogenic SO_2 of 90 Tg year^{-1} , 40% of which reacts to produce SO_4^{2-} particles covering $5 \times 10^{14} \text{ m}^2$ of the Earth's surface with a residence time of 0.02 years. Under these conditions the anthropogenic sulfate burden is $4.6 \times 10^{-3} \text{ g m}^{-2}$ (Charlson et al., 1992). With a mid-visible sulfate scattering cross-section of $5 \text{ m}^2 \text{ g}^{-1}$ at a low (30%) relative humidity, the global optical depth attributable to dry anthropogenic sulfates is $\tau_{\text{SO}_4^{2-}} \approx 0.02$. This is approximately seven times the dry

background aerosol optical depth that was calculated by Pueschel et al. (1994a) from measured size distributions in the Pacific Basin free troposphere. Allowing for a relative increase in scattering due to larger particle sizes associated with deliquescent or hygroscopic accretion of water as the relative humidity increases, the globally averaged optical depth is $\tau \approx 0.04$ (Charlson et al., 1992). This value is four times the optical depth typically measured in the free troposphere (e.g., Russell et al., 1993). The corresponding radiative transfer forcing is $\Delta F_r = -1.3 \text{ W m}^{-2}$, assuming a global top-of-the-atmosphere radiative flux of 1370 W m^{-2} , of which 76% reaches the surface given a global mean albedo of 15% through 60% cloud cover (Charlson et al., 1991).

Kiehl and Briegleb (1993) argue that a specific extinction of $5 \text{ m}^2 \text{ g}^{-1}$ is valid only for mid-visible wavelengths. It is larger for wavelengths less than $0.55 \mu\text{m}$ and decreases rapidly for wavelengths greater than $0.55 \mu\text{m}$, thereby reducing the aerosol climate forcing. They also assume an asymmetry parameter that is larger than the one used by Charlson et al. (1992). As a consequence, their radiative transfer forcing, at similar anthropogenic aerosol optical thickness, is reduced by about a factor of 2 compared with the value of Charlson et al. (1992).

Several attempts (e.g., Enghardt and Rodhe, 1993) have been made to validate climate forcing by sulfate aerosols. These have involved searching for differences in the evolution of the hemispheric annual mean temperatures that should be associated with the difference in hemispheric sulfate loadings. This comparison is made difficult because of the large difference in proportions of land and sea between the two hemispheres. Locations of polluted regions mainly over the continents in the northern hemisphere (NH) and of clean regions over the oceans in the southern hemisphere (SH) add further problems. These differences are probably also the reason why model estimates of the greenhouse effect generally indicate a more rapid warming in the NH than in the SH (e.g., Gates et al., 1992). An additional complicating factor may be the increased cloudiness observed at several continental sites in the NH (Henderson-Sellers, 1986), which is likely to be connected to a decrease in the daily annual temperature range (Karl et al., 1991). Although some of the studies indicate a smaller warming of the NH than the SH, the results so far have been inconclusive.

Opposing the cooling forcing by SO_4^{2-} and enhancing the warming potential of greenhouse gases are radiation-absorbing aerosols. Light absorption is highest for particles containing elemental black carbon (soot) produced by the incomplete combustion of carbonaceous fuel. During dust storms, soil particles (primary, natural), second only to black carbon (soot; secondary, anthropogenic) aerosol (BCA), can also make a contribution to the absorption of solar radiation in the lower atmosphere. However, it is BCA that has the highest absorption cross-section, on the order of $10 \text{ m}^2 \text{ g}^{-1}$ (Faxvog and Roessler, 1978). It dominates the absorption of light in most environments (Clarke and Charlson,

1985) and can play a role in radiative transfer and in the effects of aerosols on climate (Ackerman and Toon, 1981). In particular, it can offset the cooling effect attributed to anthropogenic sulfates (Charlson et al., 1992; Kiehl and Briegleb, 1993) and accelerate atmospheric warming by the greenhouse effect (IPCC, 1990). Charlock and Sellers (1980) estimate that if BCA decreases the albedo of aerosols, with an assumed global average of optical depth of 0.125, from 0.95 to 0.75, the radiative effect of the aerosols changes from a net cooling of -1.2°C to a net warming of 0.5°C . Pollack et al. (1976) postulate that $\varphi_0 = 0.98$ in the stratosphere changes cooling to warming.

Absorption of radiation from the Sun by tropospheric aerosols is one of the major sources of diabatic heating of as much as $5^{\circ}\text{C day}^{-1}$ in dense haze layers in the lower troposphere, thereby affecting the daytime boundary layer structure (Asano and Shiobara, 1989). Calculations performed on a radiative model of the atmosphere that incorporates dust as an absorber and scatterer of infrared radiation show an increased greenhouse effect for a reference wavelength of $0.55\ \mu\text{m}$, where the net upward flux at the surface is reduced by 10% owing to the strongly enhanced downward emission. There is a substantial increase in the cooling rate near the surface, but the mean cooling rate throughout the lower troposphere is only 10% (Harshvardhan and Cess, 1978). Total heating rates of 0.175 and $0.235\ \text{K h}^{-1}$ have been deduced for hazy and foggy atmospheres, respectively, with a new airborne radiometric system with a time resolution as high as 60 ms. The aerosol contributions to these heating rates have been found to be 0.065 and $0.235\ \text{K h}^{-1}$, respectively (Ackerman and Valero, 1984). These results indicate a possibility of aerosol absorption inhibiting local precipitation.

The $10\ \text{m}^2\ \text{g}^{-1}$ absorption cross-section for soot can be increased if soot is mixed in certain ways with other types of aerosol. Any situation from pure soot particles existing separate from transparent, e.g., $(\text{NH}_4)_2\text{SO}_4$, particles (external mixtures) through to sulfate particles incorporating some mass fraction of the soot (internal mixtures) is possible. Owing to focusing inside the sulfate, the mixed particles can absorb 2.4 times as much light as an external mixture with the same bulk chemical composition (Heintzenberg, 1978). Incorporated in sufficient amounts into cloud drops, soot aerosol can affect the cloud albedo (Twohy et al., 1989). If the BCA is located in the interior of a drop, the specific absorption coefficient for the BCA is increased from about 10 to $20\ \text{m}^2\ \text{g}^{-1}$. If the BCA particles are concentrated near the surface of the drop, the absorption coefficient may be enhanced by two to three orders of magnitude (Bhandari, 1986). Heating rates twice as high for mixed soot/transparent particles than for a population of independent soot and transparent particles with the same bulk composition have been calculated for Arctic haze (Wendling et al., 1985).

Estimates of mass ratios of SO_4^{2-} to BCA in aerosol and rain in near-source regions vary between 2 and 4 (Penner et al., 1993). Because the mid-visible

scattering cross-section of SO_4^{2-} and the absorption cross-section of BCA are nearly equal ($10\text{ m}^2\text{ g}^{-1}$) at representative relative humidities in the planetary boundary layer, these concentration ratios imply single-scattering albedo values $0.9 < \varphi < 0.95$. Additional oxidation of SO_2 downwind from sources increases the concentration of SO_4^{2-} , but not of BCA, thereby increasing the ratio of scattering to absorption. Measurements in the free troposphere yield BCA concentrations that barely reach 1% of the total aerosol. Over surfaces with low albedo ($\varphi < 0.1$ is characteristic of most of the Earth), such aerosols cool rather than warm the Earth-atmosphere system (Coakley et al., 1983). Thus the scattering by SO_4^{2-} should dominate absorption by BCA at most latitudes, but absorption can dominate at high latitudes, especially over highly reflecting snow- or ice-covered surfaces (Blanchet, 1989).

5.4.1.2. Indirect Radiative Forcing

Increased concentrations of CCNs result in increased concentrations of cloud droplets, resulting in enhanced short-wave albedo of clouds (Twomey, 1977; Coakley et al., 1983). Sulfate aerosols appear to act as major anthropogenic CCNs (Charlson et al., 1992), but particles of smoke from biomass burning may be important as CCNs in some circumstances (Penner et al., 1992). About half of the anthropogenic SO_4^{2-} particles are active as CCNs. Estimates place the CCN numbers in the northern hemisphere 30–50% above those in the southern hemisphere. A 30% increase in the number of CCNs could imply a negative climate forcing at least as large as the direct sulfate forcing (Schwartz, 1988), resulting in a total negative sulphate aerosol forcing of the same magnitude as the positive forcing due to the increases in CO_2 (1.5 W m^{-2}) and other greenhouse gases (IPCC, 1990). Such a large total sulfate aerosol forcing is incompatible with a lack of differences in hemispheric temperatures.

Radiative properties of cirrus clouds and latent heat evolution rates of convective clouds are both highly sensitive to microphysical constraints provided by nuclei from the stratosphere or the Earth's surface. Such nuclei give rise to ice particles at temperatures below 0°C and to large cloud droplets ($r > 40\ \mu\text{m}$) at temperatures both below and above 0°C at mid-levels in the atmosphere. In the troposphere at high altitudes near -40°C , cirrus crystals form on soluble H_2SO_4 which dilute to cloud droplets and freeze by homogeneous nucleation; alternatively, mineral particles advected from the surface may form crystals at somewhat higher temperatures. Incorporation of high concentrations of nuclei into regions of cirrus formation would be expected to lead to greater optical depth (more smaller crystals and greater surface area for a given mass of ice).

Because cloud droplets form by condensation of water on existing CCN particles, the concentration, size, and water solubility of CCNs have an immediate influence on the concentration, size, and chemical make-up of the cloud droplets. The short-wave radiative properties of clouds change even if the

macroscopic and thermodynamic properties of these clouds are not affected by the aerosol. In contrast, the perturbation in long-wave absorption by tropospheric clouds arising from an increase in cloud droplet concentration is negligible, because tropospheric clouds are already optically thick at infrared wavelengths (Paltridge and Platt, 1976).

A decrease in mean droplet size associated with an increase in cloud droplet concentration is expected to also inhibit precipitation development and to increase cloud lifetimes (Albrecht, 1989). Such an enhancement of cloud lifetime and the resultant increase in fractional cloud cover would increase both the short- and long-wave radiative influence of clouds. Because this effect would predominantly influence low clouds for which the short-wave influence dominates (Paltridge and Platt, 1976), the net effect would be one of further cooling. Inhibited precipitation development might further alter the amount and vertical distribution of water and heat in the atmosphere and thereby modify the Earth's hydrological cycle. Although these effects cannot yet be quantified, they have the potential of inducing major changes in global weather patterns as well as in the concentration of water vapor, the dominant greenhouse gas (Twomey, 1991).

5.4.1.3. Stratospheric Aerosol Radiative Forcing

Particulate matter normally found in the stratosphere above the tropopause may also influence the terrestrial radiation balance, catalyze heterogeneous chemical reactions, and serve as a tracer of atmospheric motion. Unaffected by volcanic eruptions, the stratospheric aerosol optical depth is too small to significantly affect the Earth's climate (Pollack et al., 1981). Enhanced stratospheric haze layers resulting from the injection of aerosol-forming material into the stratosphere by volcanic eruptions, however, can alter that pattern.

Major volcanic eruptions typically inject huge quantities of terrestrial material into the stratosphere (Lang, 1974), thereby producing primary (ash) and secondary (sulfuric acid from SO_2) aerosols. Such volcanic aerosols have long been suspected to cause short-term climate changes (Pollack et al., 1976). Because of their small (submicron) size, these aerosols are more effective at attenuation by scattering of incoming solar radiation (the albedo effect) than they are at absorbing the long-wave terrestrial radiation (the greenhouse effect). Thus the particles change the Earth's radiation balance by reflecting more of the Sun's energy back to space, at the same time permitting the planet to cool radiatively at about the same rate as before an eruption. The result is a net loss of energy for the Earth-atmosphere system or a cooling of the below-aerosol atmosphere and the surface. Because volcanic dust depletes some of the energy available to the Earth's climate system, thereby forcing the system to adapt to a new equilibrium state, the change in the Earth's radiation budget that is initiated by volcanic eruptions is termed volcanic aerosol forcing. This was observed after the 1984

eruption of the Mexican volcano El Chichon, when the solar radiation received at the surface at several locations in the US and in Hawaii was depleted by 25%, diffuse sky radiation was enhanced by up to a factor of 3, and global radiation was lowered by up to 5% (Rao and Takashima, 1986).

Volcanic aerosol-enhanced clear-sky albedos are most effective at the lowest surface albedos and decrease monotonically with increasing background albedo. For example, Valero and Pilewski (1992) show that surface albedos of 0.05 (typical for oceans) and 0.30 (characteristic for land areas) increase at $0.55 \mu\text{m}$ wavelength by 0.052 and 0.032, respectively, when a volcanic aerosol layer is inserted above the background concentration. Thus a small rise in aerosol optical depth substantially increases the Earth-atmosphere albedo over the relatively dark surfaces of the cloud-free oceans, but has a smaller or no impact on the total albedo over brighter surfaces such as clouds and light sand or alkali deserts. This means that aerosol climate forcing varies regionally and with latitude and season. However, volcanic aerosols from large eruptions generally spread over most of a hemisphere and remain airborne for about a year or more. Therefore the global (or hemispheric) mean is an appropriate case for studying the extent of climate forcing by individual volcanic eruptions.

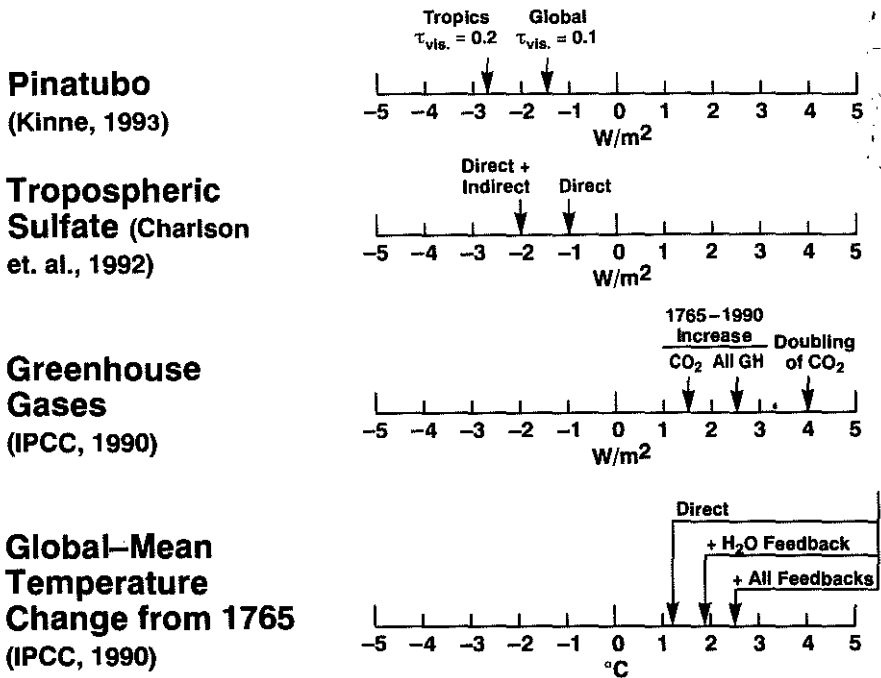
The most common method of estimating volcanic aerosol forcing is to calculate the radiative transfer on the basis of assumptions or measurements of aerosols and their properties. For example, Minnis et al. (1993) analyzed direct Earth Radiation Budget Experiment (ERBE) satellite (ERBS) measurements of the radiation budget, as well as optical properties of the aerosol, to quantify the volcanic forcing by the 1991 eruption in the Philippines of Mount Pinatubo. They compared post-Pinatubo monthly means of incoming total, reflected short-wave and outgoing long-wave radiation with the average ERBS monthly means for 1985–1989. The difference between a given post-Pinatubo monthly mean and its corresponding pre-Pinatubo 5 year monthly average is defined as an anomaly. In this way it was determined that the globally averaged anomalous radiative cooling caused by Mount Pinatubo between -40 and $+40$ degrees latitude during August and September 1991 was $-2.7 \pm 1.0 \text{ W m}^{-2}$. This estimate compares favorably with results from a theoretical model that predicts a net forcing of -2.8 W m^{-2} (Lacis et al., 1992) for a global mean of a volcanic aerosol optical depth of 0.15. Such an optical depth was actually observed after the 1991 eruption of Mount Pinatubo (Russell et al., 1993).

The influence of existing tropospheric clouds on reduction of the short-wave albedo (increased background albedo) and a decreased temperature difference between aerosol layer and emitting troposphere by stratospheric aerosols has been investigated by Kinne (1993). His calculations agree with the infrared forcing of Lacis et al. (1992), but the solar forcing is lower by about 50% owing to the presence of tropospheric clouds. Thus the net global Pinatubo volcanic aerosol forcing is about -2 W m^{-2} for the troposphere and about -1 W m^{-2} for the

Earth-atmosphere system. Figure 5.7 summarizes various aerosol climate forcings in relation to those from greenhouse gases.

The estimated global net flux changes between -1 and -3 W m^{-2} are characteristic for the time period of several months following the June 1991 eruption of Pinatubo. These may be compared with the value of $+1.25 \text{ W m}^{-2}$ for the radiative forcing due to the increase in carbon dioxide measured since the industrial revolution (IPCC, 1990), and with the estimate of -1 W m^{-2} due to a direct (non-cloud) effect of anthropogenic sulfates (Charlson et al., 1992). Thus it is clear that the Pinatubo climate forcing, similar to many other volcanic forcings, had the potential to initially offset and later delay CO_2 -induced greenhouse warming. This would be the case as long as the mid-visible optical depth exceeded about one tenth, approximately 10 times the background aerosol optical depth.

RADIATIVE FORCING OF CLIMATE*



* = Change in net (down - up; shortwave + longwave) radiative flux at tropopause

FIGURE 5.7. Pinatubo aerosol radiative forcing (Kinne, 1993), shown in relation to radiative forcing by anthropogenic sulfates (Charlson et al., 1992) and greenhouse gases (IPCC, 1990).

An influence of tropospheric clouds on volcanic aerosol forcing raises an important question of possible feedback of volcanic aerosol on these clouds. After an eruption, volcanic debris in the stratosphere enters the troposphere, primarily as a result of tall convective storms and tropopause folds. Significantly enhanced tropospheric aerosol loading attributed to Mount Pinatubo was observed by lidars as far north as 40° N during August 1991 (Post et al., 1992). These aerosols were available for incorporation into clouds, especially at the upper levels. Sulfate aerosols function as efficient cloud condensation nuclei, and volcanic ash can act as an ice nucleus at temperatures below -16°C (Mason and Maybank, 1958). Greater concentrations of cloud and ice nuclei tend to increase the number and reduce the effective radius of the hydrometeors in the cloud. At constant liquid and ice-water contents, cloud albedo increases as effective particle radius decreases. Such an indirect effect could explain the observation by Minnis et al. (1993) of increased deep convective cloud albedo for short-wave fluxes with no effect on the long-wave flux, because optically thick (high albedo) clouds are opaque to long-wave radiation. Although the indirect effects have been reported only for deep clouds, they may also occur for other cloud types. For example, diffusion of volcanic aerosols across the tropopause may alter the optical properties of high, thin cirrus clouds or enhance the generation of clouds (Sassen, 1992). Thus it appears that volcanic radiative effects are more complex than simple models that depict direct forcing by a single aerosol layer distributed uniformly over the background. Indirect effects are not now included in most climate models.

As has been observed after the 1982 El Chichon eruption (Post, 1986), sulfuric acid droplets are indeed transported from the stratosphere into the upper troposphere. This can take place by gravitational settling (if particles are larger than $0.7\ \mu\text{m}$ diameter) or dynamically by stratospheric–tropospheric exchange processes such as tropopause folding. The result is an elevated tropospheric concentration of supercooled sulfuric acid droplets (Sassen 1992). These grow by the accretion of water vapor, which is more abundant in the troposphere than in the stratosphere. The droplets can nucleate ice to increase the cirrus particle population by as much as a factor of 5, resulting in a net radiative forcing (surface warming) by as much as $8\ \text{W m}^{-2}$ (Jensen and Toon, 1992).

Potential anthropogenic perturbations of the stratospheric aerosol are possible because of aircraft and space shuttle operations. The potential effects of emissions of sulfur dioxide gas and soot granules by supersonic transport and of aluminum oxide particulates from space shuttle rocket launches on stratospheric aerosols were estimated by Turco et al. (1980). They used an interactive particle–gas model of the stratospheric aerosol layer to calculate changes due to exhaust emissions, and a radiation transport model to compute the effect of aerosol changes on the Earth's average surface temperature. They conclude that a release of small particles (soot or aluminum oxide) into the stratosphere should not lead

to a corresponding significant increase in the concentration of optically active aerosols, because increase in large particles is severely limited by rapid loss of small seed particles via coagulation. This conclusion suggests that a fleet of several hundred advanced supersonic aircraft operating daily at 20 km altitude or one space shuttle launch per week could produce a roughly 20% increase in the large-particle concentration of the stratosphere. Aerosol increases of this magnitude would reduce global surface temperature by less than 0.01 K. This conclusion is in agreement with the findings of Pollack et al. (1976), who concluded from terrestrial and radiative transfer calculations that the climate is unlikely to be affected by supersonic transport and space shuttle operations during the next several decades.

Sampling of soot particles in the stratosphere by impactors documents a current stratospheric soot mass loading of 0.6 ng m^{-3} , which is equivalent to 0.01% of the total aerosol mass after the eruption of Mount Pinatubo in 1991. This low concentration is commensurate with current air traffic, with realistic assumptions of soot emission factors by jet engines, polar route mileage flown in the stratosphere, and particle residence times in the stratosphere. Independent studies of the absorption coefficients (Pueschel et al., 1992), in combination with total extinction as, for example, measured by a sun photometer aboard the ERBE satellite in the Stratospheric Aerosol and Gas Experiment (SAGE II; Oberbeck et al., 1989), yield a current single-scatter albedo of the stratospheric aerosol of $\varphi_0 \approx 0.99 \pm 0.01$. This value is an upper limit for two reasons. First, the 1992 post-Pinatubo high sulfuric acid aerosol concentration will decay with an e-folding time of approximately 1 year, as found in previous eruptions (Post, 1986). Second, the present soot concentration is expected to double owing to planned supersonic commercial air traffic, based on expected fuel consumption and emission factors. Such an increase in aerosol black carbon is expected to decrease the single scatter albedo by 1%, which could change the sign of climate forcing from cooling to warming (Pollack et al., 1976) and increase stratospheric temperatures by several degrees (Lacis et al., 1992). Thus the 1% decrease in stratospheric aerosol single-scatter albedo due to planned supersonic commercial transport could affect tropospheric climate and significantly affect heterogeneous stratospheric chemistry (Chapter 11).

The approaches chosen to show the effect of volcanic aerosol on radiative transfer are scientifically solid, whether they are based on modelling only (e.g., Lacis et al., 1992) or on a combination of models with satellite (e.g., Minnis et al., 1993) or *in situ* observations (e.g., Kinne, 1993). Nevertheless, numerous attempts to prove an effect on air or sea surface temperature, the ultimate climate response parameter, have produced only mixed results (e.g., Angell and Korshover, 1983). The reasons are similar to those complicating the observation of an effect of tropospheric aerosols on temperature, as was discussed earlier. Volcanic forcing, in addition, is too short-lived to overcome the thermal inertia

of the the Earth's surface, particularly the oceans. Radiative transfer forcing during the immediate post-eruption period is temporary and will change with time owing to changes in the volcanic aerosol characteristics. Gravitational settling will remove the relatively large primary ash aerosols preferentially, while smaller particles stay behind and will be replenished by the generation of submicron particles due to SO_2 gas- H_2SO_4 droplet conversion for many more months after an eruption. For example, size distribution measurements after the 1991 Pinatubo eruption showed that particle size initially increased from a pre-eruption effective radius (defined as the ratio of the third and second moments of the size distribution) of approximately $0.25 \mu\text{m}$ to $0.8 \mu\text{m}$ (observed 18 months after the eruption). From then on it decreased exponentially back to $< 0.30 \mu\text{m}$ after 3.0 years following the eruption. Theoretical calculations show infrared forcing (greenhouse warming) to be a strong function of particle size, while the opposing short-wave forcing is relatively insensitive to particle size if the effective radius is larger than the effective solar wavelength (Lacis et al., 1992). Greenhouse warming relative to albedo cooling will therefore be greatest shortly after an eruption.

Only recently was it possible to pick out an overall global cooling effect of 0.1 – 0.5°C by volcanoes from the randomly fluctuating natural temperature patterns from one year to the next (Kerr, 1989). This required numerous case studies before making a link between volcanic eruptions and a particular weather pattern. The number of large eruptions in historic times is almost too sparse to build a statistically significant case, and a cooling effect of the few eruptions on record is masked by the warming due to El Niño and greenhouse gases (Mass and Portman, 1989).

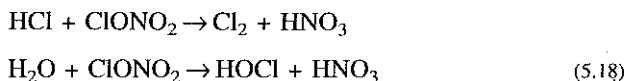
The complexity of volcanic aerosol climatic forcing is illustrated by the fact that 1991–1992 was marked by an unusually mild winter throughout North America and much of northern Eurasia, despite expected post-Pinatubo cooling (Kerr, 1993). This counter-intuitive effect of raising winter temperature in one part of the globe by altering weather patterns in another has been explained by Robock and Mao (1992). They surveyed winter temperatures at sites throughout the northern hemisphere immediately following what they estimated were the 12 largest volcanic eruptions since hemispheric records have been kept. After correcting for the climate effects of El Niño's warm Pacific waters, it was found that the winter after each eruption was unusually mild across northern Eurasia. The phenomenon is explained by surface weather patterns that are altered by the stratospheric aerosol through a chain of physical processes. First the aerosol absorbs solar radiation and warms the tropical stratosphere where sunshine is abundant even in winter. This then intensifies the stratospheric temperature difference between the tropic and polar regions, strengthening the potential vorticity of the polar vortex. This in turn redirects the jet streams below the stratosphere that guide storms. The result is a surge of warm air north into North America and northern Eurasia and of cold air down over Greenland.

5.4.2. Heterogeneous Chemistry

5.4.2.1. Stratospheric Ozone Depletion

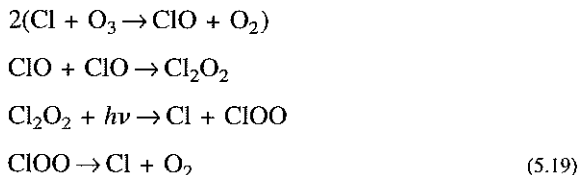
Aerosol surfaces in the atmosphere permit chemical reactions to occur which would otherwise be kinetically unfavorable. Heterogeneous reactions initiated and/or catalyzed by atmospheric particles can lead to major shifts in gas phase photochemistry.

In the stratosphere, catalysis of nitrate transformations on or in polar stratospheric cloud (PSC) particles is now proven to be capable of inverting the standard relationships between chlorine reservoirs and ClO_x radicals in the polar regions, and a direct consequence has been massive Antarctic ozone depletions. In the cold Antarctic stratosphere, particles of nitric acid n -hydrate (type I polar stratospheric clouds) first condense at about 193 K; water ice particles (type II clouds) form when the temperature falls to about 187 K (e.g., Toon et al., 1986). These polar stratospheric clouds provide surfaces for reactions that are the key to the Antarctic ozone hole (see Chapter 11). The heterogeneous reactions convert inert hydrogen chloride (HCl) and chlorine nitrate (ClONO_2) to reactive molecular chlorine (Cl_2) and hypochlorous acid (HOCl):



The molecular chlorine and hypochlorous acid are gases that can be photolyzed by solar radiation to form chlorine radicals which can catalyze ozone destruction. In contrast, the HNO_3 produced by those heterogeneous reactions remains condensed on the cloud particles. This condensation ties up the nitrogen compounds that, were they in the gaseous phase, would react with active chlorine to re-form inert ClONO_2 . During the winter, some of the relatively large type II particles have settling velocities large enough to transport the HNO_3 to lower altitudes. This process of denitrification physically separates HNO_3 from ozone-reactive Cl radicals, thereby extending the lifetime of active chlorine.

In polar spring, when the Sun reappears, photons dissociate Cl_2 into chlorine atoms (Cl) that attack ozone, yielding molecular oxygen and chlorine monoxide (ClO), which forms a dimer that also is photolyzed to Cl to destroy more ozone:



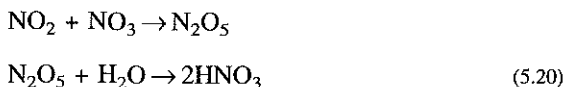
The validity of this chemical ozone depletion scheme has been verified by many studies, such as satellite observations (McCormick et al., 1989), lidar measurements (Gobbi et al., 1991), balloon observations (Deshler et al., 1992), and nitric acid-specific aerosol formation (Pueschel et al., 1989 and 1990). These workers all found nitric acid trihydrate formation at the appropriate temperatures, corresponding to concentrations of NO_x and H_2O vapors that were measured independently.

The major sources of the HCl in the stratosphere are industrial chlorine compounds such as chlorofluorocarbons (CFCs) used by man as refrigerants and aerosol propellants. CFC production has been increasing steadily since the 1950s. The 1990 Montreal Protocol forced severe restrictions on the production of chlorofluorocarbons, resulting in a leveling of atmospheric concentration (see Chapter 7 for details).

Aerosol added to the stratosphere can affect ozone concentrations in several ways. First, sunlight absorbed by the aerosol particles can heat the stratosphere, altering its usual circulation patterns (Kinne et al., 1992). Secondly, the aerosol could increase chlorine- and bromine-catalyzed ozone depletion by providing surfaces for heterogeneous reactions (Prather, 1992). Thus aerosols from Mount Pinatubo could be responsible for the increase in size of the Antarctic ozone hole this past year (Solomon et al., 1993), which was about 25% bigger than average and the largest on record. Mount Pinatubo injected 15–30 Tg of SO_2 directly into the stratosphere (Brasseur and Granier, 1992). Within several months of the eruption, stratospheric H_2SO_4 droplets had spread from the tropics to high latitudes, increasing the aerosol layer some 20–50 times over its background levels (Brock et al., 1993). Because of an exponential decay (Post, 1986), it will be several years before aerosols approach pre-Pinatubo levels.

Enhanced aerosols from volcanoes such as Mount Pinatubo are accelerating ozone depletion at high latitudes primarily through the reaction of ClONO_2 with water. Laboratory studies have shown that this reaction proceeds on dilute sulfate aerosols (Luo et al., 1993) and that the reaction rate is strongly dependent on the fraction of sulfuric acid in solution. The colder the temperature, the greater are the water content and holding capacity of HCl and the faster the reaction proceeds. Thus the ClONO_2 and H_2O are most likely to trigger extra ozone depletion in the coldest regions of the stratosphere near the poles and in the tropics.

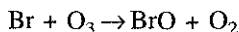
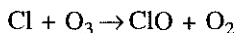
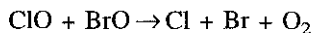
A second temperature-independent mechanism is the reaction of dinitrogen pentoxide (N_2O_5) with H_2O to form nitric acid (Rodriguez et al., 1991):



However, before this former reaction, chlorine could have been bound as follows:



The $\text{H}_2\text{SO}_4/\text{H}_2\text{O}$ aerosol removes NO_2 , allowing ClO and BrO concentrations to rise. The active halogen species can then catalytically destroy ozone:



Prather (1992) argues that an increased effective surface area of sulfuric acid after volcanic eruptions can induce heterogeneous reactions involving ClONO_2 , and secondarily N_2O_5 , to suppress NO_x abundances by more than a factor of 10 relative to gas phase chemistry. When NO_x levels fall below a threshold, e.g., 0.6 ppb at 24 km in mid-latitudes, the chlorine-catalyzed loss of O_3 proceeds at rates comparable with those during the formation of the Antarctic ozone hole, more than 50 ppb day^{-1} . Such losses might have occurred in the most volcanically perturbed regions over the tropics and mid-latitudes following the eruption of Mount Pinatubo. Various investigators (e.g., Brock et al., 1993) measured up to 20-fold increases in the stratospheric particle surface area due to the 1991 Pinatubo volcanic eruption. With a background surface area of $0.4 \mu\text{m}^2 \text{cm}^{-3}$ (Pueschel et al., 1989), the Pinatubo-enhanced volcanic aerosol surface area is close to the threshold of $10 \mu\text{m}^2 \text{cm}^{-3}$ that Prather (1992) defines as the transition region from negligible aerosol-induced ozone loss rates to those in excess of 10 ppb day^{-1} .

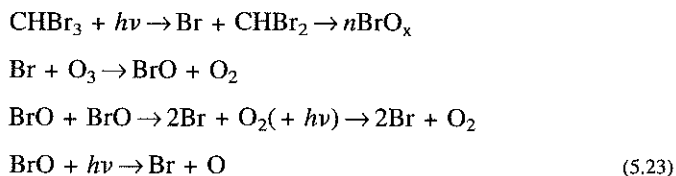
Mount Pinatubo was more than twice as effective as El Chichon in causing rapid O_3 loss, because of the increase in stratospheric chlorine (from CFCs) since 1982 (Rodriguez et al., 1991) and because overall global losses associated with a volcanic eruption are approximately linearly proportional to the amount of sulfate surface area. The build-up of atmospheric chlorine, the intensity of volcanic eruptions (Brasseur et al., 1990), and the intensity of projected aircraft emissions all play a role in the forecast of future sulfate ozone depletion.

Dustsonde-measured baseline concentrations during periods of volcanic quiescence indicate that the stratospheric background aerosol may be increasing by as much as 5–10% year^{-1} (Hofmann, 1990). Whether this increase is of natural or anthropogenic causes could not be determined because of inadequate information on sources. Carbonyl sulfide (OCS), thought to be the dominant non-volcanic and possibly anthropogenic source of stratospheric H_2SO_4 vapor (Crutzen, 1976), is especially problematic. Nevertheless, studies of catalytic destruction of ozone by anthropogenic sulfates seem to be in order. The revival

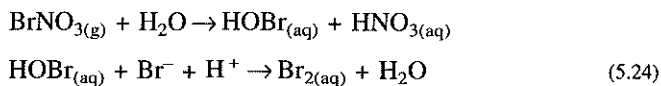
of plans for supersonic commercial aircraft promises to further enhance interest in anthropogenic (soot and sulfuric acid) aerosol-catalyzed reactions.

5.4.2.2. *Tropospheric Heterogeneous Chemistry*

Aerosol particles also play a crucial role in the depletion of ozone in surface air, as is often observed in the Arctic spring. In contrast with stratospheric chemistry, Cl plays no known role in this process. Solar radiation reaching the Earth's surface is not energetic enough to photodissociate chloroform and other chlorinated hydrocarbons (CFCs). Brominated and iodinated hydrocarbons, however, largely of oceanic origin, do absorb solar radiation at the surface sufficiently to create atomic bromine and ozone loss by the following cycle (Barrie et al., 1988):



This cycle of Br reacting with ozone, followed by the self-reaction of the BrO produced, represents a catalytic loss mechanism for O₃ as Br is regenerated. However, the radicals Br and BrO are rapidly converted to the non-radical (inert) species hydrobromic acid (HBr), hydrobromous acid (HOBr), and bromine nitrate (BrNO₃). McConnell et al. (1992) proposed that cycling of inorganic bromine between aerosols and the gas phase could maintain sufficiently high levels of Br and BrO to destroy ozone, but they did not specify a mechanism for aerosol phase production of active bromine species. Fan and Jacob (1992) proposed such a mechanism, based on known aqueous phase chemistry. It rapidly converts HBr, HOBr and BrNO₃ back to Br and BrO radicals. For example, BrNO₃ should be rapidly scavenged by the aerosol and hydrolyzed to HOBr(aq) in solution, followed by subsequent reaction of HOBr(aq) and Br⁻ to produce Br₂(aq):



As Br₂(aq) is produced, it volatilizes to the gas phase where it is photodissociated to Br. Similarly to the situation in the stratosphere, this mechanism should be particularly efficient in the presence of high concentrations of sulfuric acid aerosols that are frequently observed during boundary layer ozone depletion events.

5.5. SUMMARY AND FUTURE NEEDS

Atmospheric sulfur gases may arise either from industrial activity or from natural sources such as volcanoes and the oceans. These gases are transformed in the atmosphere to sulfate particles and/or sulfuric acid droplets. Particles reflect sunlight back to space, thus decreasing the heat input to the Earth. Potentially, the temperature of the Earth-atmosphere system is thereby lowered. The amount of sulfur emitted globally by human activities has increased from about 10 Tg year^{-1} in 1880 to about 150 Tg year^{-1} in 1990. Therefore reflection of sunlight has possibly increased, perhaps enough over time to reduce the amount of heating induced by trapping of surface infrared radiation.

Several large volcanic eruptions in the last three decades, for which the change in sunlight reaching the Earth's surface has been measured, provide proof of radiative forcing by volcanic aerosols. Although the intensity and frequency of eruptions are unpredictable, powerful eruptions generate large quantities of stratospheric sulfuric acid with e-folding times of about 1 year. As a consequence, particles spread wide enough over one or both hemispheres to globally average their effects.

In the visible it appears that an extinction exceeding $3 \times 10^{-4} \text{ km}^{-1}$ is outside 1σ error bars of measurements. Assuming an average tropopause height of 10 km, this extinction implies an optical depth of $\tau \approx 0.003$. This is close to the "background" optical depths measured with the NASA Ames autotracking airborne sun photometer at Mauna Loa, Hawaii and aboard Ames aircraft prior to the 1991 eruption of Pinatubo volcano. Therefore an anthropogenic SO_4^{2-} optical depth of $\tau \approx 0.04$, shown by Charlson et al. (1992) to yield a direct negative climate forcing of about 1 W m^{-2} , in the free troposphere would be more than 10 times the "background" optical depth of the Pacific Basin free troposphere. Such an increase in optical depth would easily be detectable with existing aerosol instruments, especially on airborne platforms where they can separate boundary layer from free tropospheric and volcanically influenced stratospheric contributions. It might be difficult, however, to delineate an anthropogenic sulfate effect within the boundary layer, where the optical depth generally exceeds 0.04.

The man-made sulfur component is SO_2 from the combustion of fossil fuel. It is injected into the boundary layer. The effects are therefore largely confined to the lower troposphere. Assessment of global effects is a difficult undertaking for several reasons. Sources of anthropogenic aerosols are not uniformly distributed. Anthropogenic particles are short-lived in the atmosphere. As a consequence, their spatial concentration is highly variable. Rates of secondary particle formation and the time evolution of the size distribution, both of which determine the aerosol optical and cloud nucleating capabilities, are dependent on the production of condensable material and the concentration and size distribution of

aerosol particles already present. Aerosol formation and removal processes are covariant with diurnally, synoptically, and seasonally varying features of the Earth-atmosphere system. A task that appears in order is screening of historic optical depth data for trends that would be proportional to the trend in atmospheric sulfur emissions.

Large gaps exist in the knowledge of anthropogenic aerosols, preventing quantification of their influence for use in climate models. What is needed is a coupling of (1) the physical-chemical processes that produce them and the meteorological processes that distribute and remove them with (2) the physical and optical characteristics that determine radiative transfer and cloud microphysical effects.

Globally representative measurements of aerosol and cloud properties may conceivably be obtained by satellites equipped with photopolarimeters to measure the radiance and polarization of reflected sunlight in the spectral range from the near ultraviolet to the near infrared (Hansen et al., 1990). Specific cloud properties such as height, optical depth, particle phase, and effective size may also be derived from satellites. However, validation and improvement of inferences drawn from satellite measurements require that such satellite monitoring be tied to concurrent ground-based and *in situ* aircraft measurements of optical and microphysical cloud and aerosol parameters. This is particularly true for the vertical inhomogeneities, because satellites (like ground-based measurements) provide only height-integrated values of the aerosol parameters. Nevertheless, vertical distribution information is required, because effects of light scattering and absorption are altitude-dependent, as are cloud properties. The climatic effect (heating versus cooling) depends on the ambient temperature of an aerosol of given scattering/absorption characteristics.

During periods of volcanic quiescence, stratospheric aerosol formation processes depend on transport. Unfortunately, there is much uncertainty regarding the meridional transport of the stratospheric gases and particles. It is possible that the aerosols themselves could be used as tracers. In the winter of 1982-1983 the northward transport rate of El Chichon aerosols was observed by six lidars stationed between 19° and 55° latitude. The transport rate of the cloud maximum was estimated to be approximately $0.3^\circ \text{ day}^{-1}$, and on January 1, 1983 it was located near 30° N. Within the uncertainty of the measurements, the cloud maximum optical thickness appeared to remain constant with latitude. On the other hand, the stratospheric aerosol concentration at 40° N began to rise a few weeks after the eruption. Nearly identical transport behavior was observed from sun photometer data following the eruption of Agung.

Thus a lidar network consisting of perhaps 20 lidars over a region perhaps as large as the United States could determine the latitudinal transport of stratospheric aerosols after volcanic eruptions. If the system were operated in some sort of unmanned mode with identical lasers and data reduction schemes,

one should be able to obtain an excellent picture of stratospheric motions. In particular, tropopause fold events could be studied, with a view toward measuring the fluxes of water vapor, sulfur compounds, and particulates into the stratosphere, as well as the downward flux of stratospheric aerosols as a potential source of nuclei for upper tropospheric cirrus cloud particles.

The mean circulation of the quasi-biennial oscillation strongly affects the distribution of aerosols. The associated presence or absence of a subtropical barrier in potential vorticity will discourage or allow transport of aerosols out of the tropics by extratropical Rossby waves. The time evolution of volcanic veils may be used to infer the morphology of the potential vorticity barrier.

Aerosol composition is a strong function of air parcel history. Chemical general circulation models (GCMs) may soon be capable of representing the overlap of tracer tongues, but at present this is limited by computational capabilities. To form aerosols containing constituents with different geographical sources probably requires differential air mass advection in the vertical, coupled with small scale mixing due to gravity waves. GCMs are still a long way from being able to represent these small scale mixing processes adequately.

In the discipline of atmospheric chemistry, mechanisms of the heterogeneous reactions are only beginning to draw attention but are at the heart of several critical environmental problems. Chlorine activation is known to take place on stratospheric particle surfaces at the poles and potentially in other localities. Bromine activation has been shown to occur in surface air in the Arctic. Aspects of aerosol physical chemistry underpin the heterogeneous mechanistic. Compositions, vapor pressures, and (in the PSC instance) adsorption equilibria all pertain to aerosol reactivities. They are all influenced by particle surface characteristics. Fundamental physical properties, including morphologies and size distributions, also enter into the determination of heterogeneous reaction rates. Optical phenomena are central to the measurement of these properties. The process of nucleation, through which the aerosols under consideration are formed originally, remains obscure at all stages for polar stratospheric clouds.

The following paragraphs offer a list of topics for which major questions are outstanding regarding the influence of atmospheric particles on chemistry, along with a set of suggestions for relevant experiments, including laboratory, *in-situ*, and numerical approaches. The major thrust is toward the PSCs because they are of immediate and critical concern, but many of the overall concepts apply to sulfate as well. The problems presented are subdivided into sections focusing on the physical chemistry of heterogeneous reactions, aerosol properties bearing on them, and fundamental microphysical issues such as nucleation. Some broader-scale objectives for future polar field campaigns are also discussed.

Composition of polar stratospheric clouds is perhaps the most basic facet of their physical chemistry. It determines nitrate reactivity but remains poorly understood on several key levels. For example, nitric acid trihydrate (NAT),

which probably comprises the bulk of type I PSC material, can exist under a wide range of water concentrations. The water mole fraction in turn specifies HCl holding capacities, and efficiencies for the reaction between nitrate and HCl. Actual water concentrations in the NAT particle, however, remain unknown. *In situ* mass spectroscopy of the type I PSC contents is a possibility, and it may be possible to obtain rough measurements of solid phase $\text{H}_2\text{O}/\text{HNO}_3$ ratios. *In situ* infrared spectroscopy of the type I clouds could also provide clues to their composition but would have to be preceded by laboratory documentation of NAT absorption bands. A third possibility is to capture PSC crystals and analyze them wet chemically for the same information, but their ease of evaporation makes this a difficult task.

Solid vapor pressures are linked closely to composition, but our understanding of PSC vapor pressures is again incomplete. Effects of impurities, coatings and co-condensation of water and NAT have not been investigated. While partial pressures of H_2O and HNO_3 are available for NAT alone, they have not been correlated in detail with the water concentration of the lattice. Adsorptive thermodynamics is a theme related to PSC vapor pressures. An adsorption equilibrium constant defines the tendency for a molecule, particularly a heterogeneously active nitrate or acid, to cover a cloud particle surface. The equilibrium can in turn be converted into a surface-binding enthalpy, which enters into calculation of rates for several elementary steps occurring early in the surface reaction process. These include desorption and two-dimensional diffusion. It could be profitable to undertake determination of adsorption isotherms for the PSC heterogeneous reactants on NAT and ice. Preliminary values have already been reported for HCl (Elliot et al., 1990) and reflect formation of two hydrogen bonds with the crystal. Nitric acid adsorption might also be measurable, but values for nitrates would be complicated by competition from surface reactions.

Although a growing body of circumstantial evidence involving Lagrangian photochemical models points to type I particles as the chief chlorine activators, the PSC/ ClO_x connection merits strengthening. In the laboratory, continued effort is needed in measuring collisional efficiencies for nitrate reactions on simulated PSC materials. Early experiments were plagued by improper characterization of solids. Studies of $\text{ClONO}_2 + \text{HCl}$ on water ice, for example, were conducted at pressures orders of magnitude above the stability threshold for hydrochloric acid hydrates. NAT efficiencies may be more realistic at the moment, but the dependence of reactivity on HCl solubilities is not well established and, as mentioned above, stratospheric HCl mole fractions cannot yet be predicted with confidence. Aerosol chlorine activation could perhaps be verified directly by monitoring air upstream and downstream from a single cloud.

The possibility exists that certain subtleties of heterogeneous chemistry are being overlooked because attention has centered on the net chlorine-activating

reactions of ClONO_2 and N_2O_5 . ClO dimerization, for example, may be augmented on PSC surfaces, and as the rate controlling step in an odd-oxygen removal cycle, this recombination is clearly distinct from the nitrate transformations. HO_x species and their reservoirs are decoupled to some extent from the chlorine and nitrogen balances which limit ozone lifetimes, and so heterogeneous interactions of the hydrogen families remain unexplored. It could be instructive to systematize the thermodynamic and kinetic features required for significant heterogeneous catalysis of a gas phase reaction. The ramifications of candidate processes thus highlighted could be tested by photochemical simulation. Another logical priority is detailed bridging of polar photochemical and microphysical calculations through a conceptual model of PSC surface processes.

Of the particle characteristics that bear on heterogeneous chemistry, shape is an obvious physical property which contributes to the reactivity of nitrates or acids on stratospheric aerosols. An irregular surface exhibiting hopper characteristics or graininess will add to the available heterogeneous transformation area. Ice replicator samples have provided evidence that type II polar water ice particles are hexagonal and columnar (Goodman et al., 1989). Those type II particles had a surface area that was only 10% of the total aerosol surface area. They were, however, unexpectedly large and might effectively dehydrate the stratosphere by sedimentation. Departures from the familiar hexagonal-columnar habit are possible at different temperatures but have not been catalogued. Type I clouds have not been intensely scrutinized. Lidar depolarization data have, however, recently permitted discrimination of two new type I particle categories (Browell et al., 1990), perhaps corresponding to diverging morphologies.

Shape is in addition a function of the thermophysical aerosol state. Although polar air lies well below fusion temperatures for liquid water or aqueous nitric acid, there is the possibility of freezing point depression by unidentified impurities. It might be advisable to verify that the PSCs actually exist as solids. Vapor samples near the condensation point could be cooled under controlled conditions and the particle formation process observed, either in the laboratory or perhaps even *in situ*. Particle size is a related matter and further monitoring of the sizes of mid-latitude polar stratospheric aerosols is essential.

Particle optical effects are critical in calibration and operation of optical particle counters used to study aerosols, and consequently there is considerable interest in the accuracy with which they can determine particle characteristics, which in turn strongly depends on shape and refractive index of the particles. Dependence of refractive index on composition has not been delineated for PSC materials, and theoretical calculations would be desirable for the optical properties of non-spherical particles. Infrared spectroscopy of the type I clouds could also be classified under this heading.

Major uncertainties permeate calculations of atmospheric aerosol production, especially with regard to energy barriers against nucleation. It is currently

thought that background sulfate aerosols entering the polar stratosphere act as nuclei for type I PSCs, and type I in turn for type II. Laboratory measurements of the saturation ratio necessary to achieve particle formation could improve the modeling situation for each step in this sequence. The initial background sulfate nuclei are present in the mid-latitude stratosphere as liquid, and it has been presumed that the strong supercooling to which they are subjected in the polar vortices results in freezing. This is only conjecture, however, and laboratory or *in situ* verification could be enlightening.

Acknowledgments

This article started with a literature search that produced close to 1000 references. I scanned most of them and used many. I would like to thank all these authors for their contributions. My particular thanks go to Patrick Hamill and Scott Elliott, who contributed sections on stratospheric aerosols and on heterogeneous chemistry of the stratosphere, respectively, to a workshop report that I edited and from which I drew material for this article. A second local source is a series of proposals that I wrote during the past 8 years, notably with Phil Russell as co-proposer, to whom, therefore, I owe much of the material presented. Last but not least, I want to thank Kenneth Snetsinger for editorial comments and Hanwant Singh for his encouragement in writing this chapter.

References

- Ackerman, T.P. and Toon, O.B. (1981). Absorption of visible radiation in atmospheres containing mixtures of absorbing and nonabsorbing particles. *Appl. Opt.* **20**, 3661–3668.
- Ackerman, T.P. and Valero, F.P.J. (1984). The vertical structure of Arctic haze as determined from airborne net-flux radiometer measurements. *Geophys. Res. Lett.*, **11**, 469–472.
- Albrecht, B.A. (1989). Aerosols, cloud microphysics, and fractional cloudiness. *Science*, **245**, 1227–1230.
- Angell, J.K. and Korshover, J. (1983). Global temperature variations in the troposphere and stratosphere, 1958–1982. *Mon. Weather Rev.*, **111**, 901–921.
- Asano, S. and Shiobara, M. (1989). Aircraft measurements of the radiative effects of tropospheric aerosols. I. Observational results of the radiation budget. *J. Meteorol. Soc. Jpn.*, **67**, 847–861.
- Bach, W. (1976). Global air pollution and climatic change. *Rev. Geophys.*, **14**, 429–474.
- Barrie, L.A., Bottenheim, J.W., Schnell, R.C., Crutzen, P.J. and Rasmussen, R.A. (1988). Ozone destruction and photochemical reactions at polar sunrise in the lower Arctic atmosphere. *Nature*, **334**, 138–141.
- Bates, T.S., Lamb, B.K., Guenther, A., Dignon, J. and Stoiber, R.E. (1992). Sulfur emissions to the atmosphere from natural sources. *J. Atmos. Chem.*, **14**, 315–338.

- Bhandari, R.A. (1986). Specific absorption of a tiny absorbing particle embedded within a nonabsorbing particle. *Appl. Opt.*, **25**, 3331–3333.
- Blanchet, J.P. (1989). Toward estimation of climatic effects due to Arctic aerosols. *Atmos. Environ.*, **32**, 2609–2625.
- Blanchet, J.P. and List, R. (1983). Estimation of optical properties of Arctic haze using a numerical model. *Atmos.-Ocean*, **21**, 444–464.
- Brasseur, G. and Granier, C. (1992). Mount Pinatubo aerosols, chlorofluorocarbons, and ozone depletion. *Science*, **257**, 1239–1242.
- Brasseur, G.P., Granier, C. and Walters, S. (1990). Future changes in stratospheric ozone and the role of heterogeneous chemistry. *Nature*, **348**, 626–628.
- Brock, C.A., Jonsson, H.H., Wilson, J.C., Dye, J.E., Baumgardner, D., Borrmann, S., Pitts, M.C., Osborne, M., DeCoursey, R.J. and Woods, D.C. (1993). Relationships between optical extinction, backscatter and aerosol surface and volume in the stratosphere following the eruption of Mt. Pinatubo. *Geophys. Res. Lett.*, in press.
- Browell, E.K., Butler, C.F., Ismail, S., Robinette, P.A., Carter, A.F., Higdon, N.S., Toon, O.B., Schoeberl, M.R., and Tuck, A.F. (1990). Airborne lidar observations in the wintertime arctic stratosphere: polar stratospheric clouds. *Geophys. Res. Lett.*, **17**, 385–388.
- Burley, J.D. and Johnston, H.S. (1992). Nitrosyl sulfuric acid and stratospheric aerosols. *Geophys. Res. Lett.*, **19**, 1363–1366.
- Butcher, S.S. and Charlson, R.J. (1972). *An Introduction to Air Chemistry*, Academic Press, New York, NY.
- Charlock, T.P. and Sellers, W.D. (1980). Aerosol effects on climate: calculations with time-dependent and steady state radiative–convective models. *J. Atmos. Sci.*, **37**, 1327–1341.
- Charlson, R.J., Langner, J., Rodhe, H., Leovy, C.B. and Warren, S.G. (1991). Perturbation of the northern hemisphere radiative balance by backscattering from anthropogenic sulfates. *Tellus*, **43AB**, 152–163.
- Charlson, R.J., Lovelock, J.E., Andreae, M.O. and Warren, S.G. (1987). Oceanic phytoplankton, atmospheric sulfur, cloud albedo and climate. *Nature*, **326**, 655–661.
- Charlson, R.J., Schwartz, S.E., Hales, J.M., Cess, R.D., Coakley, J.A., Jr., Hansen, J.E. and Hofmann, D.J. (1992). Climate forcing by anthropogenic aerosols. *Science*, **255**, 423–430.
- Clarke, A.D. and Charlson, R.J. (1985). Radiative properties of the background aerosol-absorption component of extinction. *Science*, **229**, 263–265.
- Coakley, J.A. Jr., Cess, R.D. and Yurevich, F.B. (1983). The effect of tropospheric aerosols on the earth's radiation budget: a parameterization for climate models. *J. Atmos. Sci.*, **40**, 161–171.
- Crutzen, P.J. (1976). The possible importance of CSO for the sulfate layer of the stratosphere. *Geophys. Res. Lett.*, **3**, 73–76.
- Deshler, T., Adriani, A., Gobbi, G.P., Hofmann, D.J., DiDonfrancesco, G. and Johnson, B.J. (1992). Polar stratospheric clouds over McMurdo, Antarctica, during the 1991 spring: lidar and particle counter measurements. *Geophys. Res. Lett.*, **19**, 1819–1822.
- Elliott, S., Turco, R.P., Toon, O.B. and Hamill, P. (1990). Incorporation of stratospheric acids into water ice. *Geophys. Res. Lett.*, **17**, 425–428.
- Enghardt, M. and Rodhe, H. (1993). A comparison between patterns of temperature trends

- and sulfate aerosol pollution, *Geophys. Res. Lett.*, **20**, 117–120.
- Erickson, E. (1959). The yearly circulation of chloride and sulfur in nature: meteorological, geochemical and petrological implications. *Tellus*, **11**, 375–403.
- Fan, S.M. and Jacob, D.J. (1992). Surface ozone depletion in Arctic spring sustained by bromine reactions on aerosols. *Nature*, **359**, 522–524.
- Farlow, N.H., Snetsinger, K.G., Hayes, D.M., Lem, H.Y. and Tooer, B.M. (1978). Nitrogen–sulfur compounds in stratospheric aerosols. *J. Geophys. Res.*, **83**, 6207–6211.
- Faxvog, F.R. and Roessler, D.M. (1978). Carbon aerosol visibility versus particle size distributions. *Appl. Opt.*, **17**, 3859–3862.
- Friedlander, S.K. (1970). The self-preserving particle size distribution for coagulation by Brownian motion—Smoluchowski coagulation and simultaneous Maxwellian condensation. *J. Aerosol Sci.*, **1**, 115–123.
- Gates, W.L., Mitchell, J.F.B., Boer, G.J., Cubasch, U. and Meleshko, V.P. (1992). Climate modelling, climate prediction and model validation. In Houghton, J.T., Callander, B.A. and Varney, S.K., Eds., *IPCC, The supplementary Report*, Cambridge University Press, Cambridge, pp. 97–134.
- Gobbi, G.P., Adriani, A., Deshler, T. and Hoffman, D.J. (1991). Evidence for denitrification in the 1990 Antarctic spring stratosphere. I—Lidar and temperature measurements. II—Lidar and aerosol measurements. *Geophys. Res. Lett.*, **18**, 1995–2002.
- Goodman, J., Toon, O.B., Pueschel, R.F., Snetsinger, K.G. and Verma, S. (1989). Antarctic stratospheric ice crystals. *J. Geophys. Res.*, **94**, 16449–16458.
- Hansen, J., Rossow, W. and Fung, I. (1990). The missing data on global climate change. *Iss. Sci. Technol.*, **7**, 62–69.
- Harshvardhan, M.R. and Cess, R.D., (1978). Effect of tropospheric aerosols upon atmospheric infrared cooling rates. *J. Quantum Spectrosc. Radiat. Transfer*, **19**, 621–632.
- Heintzenberg, J. (1978). Light scattering parameters of internal and external mixtures of soot and nonabsorbing material in the atmospheric aerosol. *Proc. Conf. on Carbonaceous Particles in the Atmosphere, CONF-7803101*, Berkeley, CA, pp. 278–281.
- Henderson-Sellers, A. (1986). Increasing cloud in a warming world. *Climatic Change*, **9**, 267–309.
- Hicks, B.B. (1986). Differences in wet and dry particle deposition parameters between north America and Europe. In Lee, S.D., Schneider, T., Grant, L.D. and Verkerk, P.J., Eds., *Aerosols*, Lewis Publ., Chelsea, MI, pp. 973–982.
- Hidy, G.M. (1973). Removal processes of gaseous and particulate pollutants. In Rasool, S.I., Ed., *Chemistry of the Lower Atmosphere*. Plenum, New York, NY, pp. 121–176.
- Hofmann, D.J. (1990). Increase in the stratospheric background sulfuric acid aerosol mass in the past 10 years. *Science*, **248**, 996–1000.
- IPCC (Intergovernmental Panel on Climate Change) (1990). *The Scientific Assessment*, Houghton, J.T., Jenkins, G.T. and Ephraums, J.J., Eds., Cambridge University Press, Cambridge.
- Iversen, T.B.N., Halvorsen, N.E., Mylona, S. and Sandnes, H. (1991). Calculating budgets for airborne acidifying components in Europe, 1985, 1987, 1989, and 1990. *EMEP/ MSC-W Report 1/91*, Norwegian Meteorological Institute, Oslo.

- Jaenicke, R. (1986). Physical characterization of aerosols. In Lee, S.D., Schneider, T., Grant, L.D. and Verkerk, P.J., Eds., *Aerosols*, Lewis Publ., Chelsea, MI, pp. 97–106.
- Jensen, E.J. and Toon, O.B. (1992). The potential effects of volcanic aerosols on cirrus cloud microphysics. *Geophys. Res. Lett.*, **19**, 1759–1762.
- Junge, C.E. (1961). Vertical profiles of condensation nuclei in the stratosphere. *J. Meteorol.*, **18**, 501–509.
- Junge, C.E. and Gustafson, P.E. (1957). On the distribution of seasalt over the United States and its removal by precipitation. *Tellus*, **9**, 164–173.
- Karl, T.R., Kukla, G., Razuvaev, V.N., Changery, M.J., Quayle, G., Heim, R.R. Jr., Easterling, D.R. and Fu, C.B. (1991). Global warming: Evidence for asymmetric diurnal temperature change. *Geophys. Res. Lett.*, **18**, 2253–2256.
- Kerr, R.A. (1989). Volcanoes can muddle the greenhouse. *Science*, **245**, 127–128.
- Kerr, R.A. (1993). Volcanoes may warm locally while cooling globally. *Science*, **260**, 1232.
- Kiang, C.S., Cadle, R.D. and Yue, G.K. (1975). $\text{H}_2\text{SO}_4\text{-HNO}_3\text{-H}_2\text{O}$ ternary aerosol formation mechanism in the stratosphere. *Geophys. Res. Lett.*, **2**, 41–44.
- Kiehl, J.T. and Briegleb, B.P. (1993). The relative roles of sulfate aerosols and greenhouse gases in climate forcing. *Science*, **260**, 311–314.
- Kinne, S.A. (1993). Personal communication.
- Kinne, S.A., Toon, O.B. and Prather, M.J. (1992). Buffering of stratospheric circulation by tropical ozone: a Pinatubo case study. *Geophys. Res. Lett.*, **19**, 1927–1930.
- Köhler, H. (1926). Zur Kondensation an hygroskopischen Kernen und Bemerkungen über das Zusammenfließen der Tropfen. *Meddn. St. met.-hydrogr. Anst.*, **3**, 24–30.
- Kondratyev, K. (1986). *Changes in global climate*, Balkema, Rotterdam.
- Lacis, A., Hansen, J. and Sato, M. (1992). Climate forcing by stratospheric aerosols. *Geophys. Res. Lett.*, **19**, 1607–1610.
- Lang, L.J., Ed. (1974). *The World Almanac*, Newspaper Enterprise Assoc., Cincinnati, OH, pp.428–429.
- Langner, J., Rodhe H., Crutzen, P.J. and Zimmerman, P. (1992). Anthropogenic influence on the distribution of tropospheric sulfate aerosol. *Nature*, **359**, 712–716.
- Ludwig, J.H., Morgan, G.B. and McMullen, T.B. (1970). Trends in urban air quality. *EOS Trans. AGU*, **51**, 468–475.
- Luo, B.P., Clegg, S.L., Peter, Th., Mueller, R. and Crutzen, P.J. (1993). HCl solubility and liquid diffusion in aqueous sulfuric acid under stratospheric conditions. *Geophys. Res. Lett.*, in press.
- McConnell, J.C., Henderson, G.S., Barrie, L., Bottenheim, J., Niki, H., Langford, C.H. and Templeton, E.M.J. (1992). Photochemical bromine production implicated in Arctic boundary-layer ozone depletion. *Nature*, **355**, 150–152.
- McCormick, M.P., Trepte, C.R. and Pitts, M.C. (1989). Persistence of polar stratospheric clouds in the southern polar region. *J. Geophys. Res.*, **D94**, 11,241–11,251.
- Mason, B.J., (1971). *The Physics of Clouds*, Clarendon Press, Oxford.
- Mason, B.J. and Maybank, J. (1958). Ice nucleating properties of some natural mineral dusts. *Q. J. Meteorol. Soc.*, **86**, 235–241.
- Mass, C.F. and Portman, D.A. (1989). Major volcanic eruptions and climate: a critical evaluation. *J. Climatol.*, **2**, 566.
- Mayewski, P.A., Lyons, W.B., Spencer, M.J., Twickler, M.S., Buck, C.F. and Whitlow, S.

- (1990). An ice core record of atmospheric response to anthropogenic sulphate and nitrate. *Nature*, **346**, 554–556.
- Minnis, P., Harrison, E.F., Stowe, L.L., Gibson, G.G., Denn, F.M., Doelling, D.R. and Smith, W.L. Jr. (1993). Radiative climate forcing by the Mount Pinatubo eruption. *Science*, **259**, 1411–1415.
- Neftel, A., Beer, J., Oeschger, H., Zuercher, F. and Finkel, R.J. (1985). Sulphate and nitrate concentrations in snow. *Nature*. **313**, 611–613.
- Oberbeck, V.E., Livingston, J.M., Russell, P.B., Pueschel, R.F., Rosen, J.N., Osborne, M.T., Kritz, M.A., Snetsinger, K.G. and Ferry, G.V. (1989). SAGE II aerosol validation: selected altitude measurements, including particle micrometeorological measurements. *J. Geophys. Res.*, **94**, 8367–8380.
- Paltridge, G.W. and Platt, M.R. (1976). *Radiative Processes in Meteorology and Climatology*, Elsevier, Amsterdam.
- Penner, J.E., Dickinson, R.E. and O'Neill, C.A. (1992). Effects of aerosol from biomass burning on the global radiation budget. *Science*, **256**, 1432.
- Penner, J.E., Eddleman, H. and Novakov, T. (1993). Towards the development of a global inventory for black carbon emissions. *Atmos. Environ.*, **27A**, 1277–1295.
- Pollack, J.B., Toon, O.B., Sagan, C., Summers, A., Baldwin, B. and Van Camp, W. (1976). Volcanic explosions and climatic change: a theoretical assessment. *J. Geophys. Res.*, **81**, 1071–1083.
- Pollack, J.R., Toon, O.B. and Wiedman, D. (1981). Radiative properties of the background stratospheric aerosols and implications for perturbed conditions. *Geophys. Res. Lett.*, **8**, 26–28.
- Post, M.J. (1986). Atmospheric purging of ElChichon debris. *J. Geophys. Res.*, **91**, 5222–5228.
- Post, M.J., Grund, C.J., Langford, A.O. and Proffitt, M.H. (1992). Observations of Pinatubo ejecta over Boulder, Colorado by lidars of three different wavelengths. *Geophys. Res. Lett.*, **19**, 195–198.
- Prather, M. (1992). Catastrophic loss of stratospheric ozone in dense volcanic clouds. *J. Geophys. Res.*, **97**, 10187–10191.
- Prospero, J.M. and Carlson, T.N. (1972). Vertical and areal distribution of Saharan dust over the western equatorial North Atlantic Ocean. *J. Geophys. Res.*, **77**, 5255–5265.
- Pruppacher H.R. and Klett, J.D. (1978). *Microphysics of Clouds and Precipitation*. Reidel, Dordrecht.
- Pueschel, R.F., Blake, D.F., Snetsinger, K.G., Hansen, A.D.A., Verma, S. and Kato, K. (1992). Black carbon (soot) aerosol in the lower stratosphere and upper troposphere. *Geophys. Res. Lett.*, **19**, 1659–1662.
- Pueschel, R.F., Snetsinger, K.G., Goodman, J.K., Toon, O.B., Ferry, G.V., Oberbeck, V.R., Livingston, J.M., Verma, S., Fong, W., Starr, W.L. and Chan, K.R. (1989). Condensed nitrate, sulfate and chloride in Antarctic stratospheric aerosols. *J. Geophys. Res.*, **94**, 11271–11284.
- Pueschel, R.F., Snetsinger, K.G., Hamill, P., Goodman, J.K. and McCormick, M.P. (1990). Nitric acid in polar stratospheric clouds—similar temperature of nitric acid condensation and cloud formation. *Geophys. Res. Lett.*, **17**, 429–432.
- Pueschel, R.F., Livingston, J.M., Ferry, G.V. and DeFelice, T.E. (1994a). Aerosol abundances and optical characteristics in the Pacific Basin free troposphere. *Atmos.*

- Environ.*, **28**, 951–960.
- Pueschel, R.F., Russell, P.B., Allen, D.A., Ferry, G.V., Snetsinger, K.G., Livingston, J.M. and Verma, S. (1994b). Physical and optical properties of the Pinatubo volcanic aerosol: aircraft observations with impactors and a Sun-tracking photometer. *J. Geophys. Res.*, **99**, 12915–12922.
- Rao, C.R.N. and Takashima, T., (1986). Solar radiation anomalies caused by the El Chichon volcanic cloud. *Q. J. R. Meteorol. Soc.*, **112**, 1111–1126.
- Robock, A. and Mao, J. (1992). Winter warming from large volcanic eruptions. *Geophys. Res. Lett.*, **19**, 2505–2509.
- Rodriguez, J.M., Ko, M.K. and Sze, N.D. (1991). Role of heterogeneous conversion of N_2O_5 on sulphate aerosols in global ozone losses. *Nature*, **353**, 134–137.
- Russell, P.B., Livingston, J.M., Dutton, E.G., Pueschel, R.F., Reagan, J.A., DeFoor, T.E., Box, M.A., Allen, D., Pilewski, P., Herman, B.M., Kinne, S.A. and Hofman, D.J. (1993). Pinatubo and pre-Pinatubo optical depth spectra: Mauna Loa measurements, comparisons, inferred particle size distributions, radiative effects, and relationship to lidar data. *J. Geophys. Res.*, **D98**, 22969–22985.
- Sassen, K. (1992). Evidence of liquid-phase cirrus cloud formation from volcanic aerosols: climate implications. *Science*, **257**, 516–519.
- SCEP (1970). Report of the study of critical environmental problems. In *Man's Impact on the Global Environment*, MIT Press, Cambridge, MA.
- Schwartz, S.E. (1988). Are global cloud albedo and climate controlled by marine phytoplankton? *Nature*, **336**, 441–445.
- Schwartz, S.E. (1989). Acid deposition: unraveling a regional phenomenon. *Science*, **243**, 753–763.
- Sigurdsson, H. and Laj, P. (1992). In Nierenberg, W.A., Ed., *Encyclopedia of Earth Systems Science*, Vol. 1, Academic Press, San Diego, CA, p. 183.
- Solomon, S., Sanders, R.W., Garcia, R.R. and Keys, J.G. (1993). Increased chlorine dioxide over Antarctica caused by volcanic aerosol from Mount Pinatubo. *Nature*, **363**, 245–248.
- Tang, I.N., Munkelwitz, H.R. and Davis, J.G. (1977). Aerosol growth studies. *J. Aerosol Sci.*, **8**, 149–159.
- Toon, O.B., Hamill, P., Turco, R.P. and Pinto, J. (1986). Condensation of HNO_3 and HCl in the winter polar stratosphere. *Geophys. Res. Lett.*, **13**, 1284–1287.
- Turco, R.P. (1992). Upper atmosphere aerosols: Properties and natural cycles. In *The Atmospheric Effects of Stratospheric Aircraft: A First Program Report*, NASA Ref. Pub. 1272, pp. 63–82.
- Turco, R.P., Whitten, R.C., Toon, O.B., Pollack, J.B. and Hamill, P. (1980). OCS, stratospheric aerosols and climate. *Nature*, **283**, 283–286.
- Twohy, C.H., Clarke, A.D., Warren, S.G., Radke, L.F. and Charlson, R.J. (1989). Light-absorbing material extracted from cloud droplets and its effect on cloud albedo. *J. Geophys. Res.*, **94**, 8623–8631.
- Twomey, S. (1977). *Atmospheric Aerosols*, Elsevier, New York.
- Twomey, S. (1991). Aerosols, clouds and radiation. *Atmos. Environ.*, **25A**, 2435–2442.
- Valero, F.P.J. and Pilewski, P. (1992). Latitudinal survey of spectral optical depths of the Pinatubo volcanic cloud: derived particle sizes, columnar mass loadings, and effects on planetary albedo. *Geophys. Res. Lett.*, **19**, 163–166.

- Wendling, P., Wendling, R., Renger, W., Covert, D., Heintzenberg, J. and Moerl, P. (1985). Calculated radiative effects of Arctic haze during a pollution episode in spring 1983 based on ground-based and airborne measurements. *Atmos. Envir.*, **19**, 2181–2193.
- Whitby, K.T. (1978). The physical characteristics of sulfur aerosols. *Atmos. Environ.*, **12**, 135–159.
- Williamson, S.J. (1973). *Fundamentals of Air Pollution*, Addison-Wesley, Reading, MA.
- World Resources Institute and the International Institute for Environment and Development (1988). *World Resources 1988–89*, Basic Books, New York, NY.
- Yue, G.K. and Deepak, A. (1982). Temperature dependence of the formation of sulfate aerosols in the stratosphere. *J. Geophys. Res.*, **87**, 3128–3134.